

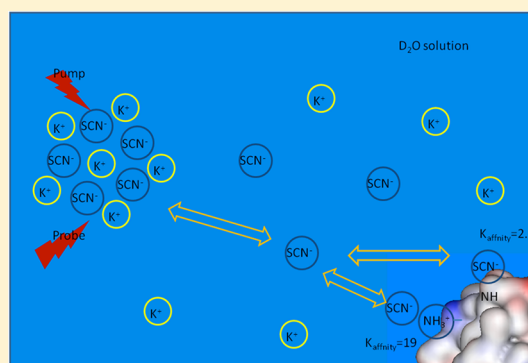
Probing Ion/Molecule Interactions in Aqueous Solutions with Vibrational Energy Transfer

Jiebo Li, Hongtao Bian, Xiewen Wen, Hailong Chen, Kaijun Yuan, and Junrong Zheng*

Department of Chemistry, Rice University, Houston, Texas 77005, United States

S Supporting Information

ABSTRACT: Interactions between model molecules representing building blocks of proteins and the thiocyanate anion, a strong protein denaturant agent, were investigated in aqueous solutions with intermolecular vibrational energy exchange methods. It was found that thiocyanate anions are able to bind to the charged ammonium groups of amino acids in aqueous solutions. The interactions between thiocyanate anions and the amide groups were also observed. The binding affinity between the thiocyanate anion and the charged amino acid residues is about 20 times larger than that between water molecules and the amino acids and about 5–10 times larger than that between the thiocyanate anion and the neutral backbone amide groups. The series of experiments also demonstrates that the chemical nature, rather than the macroscopic dielectric constant, of the ions and molecules plays a critical role in ion/molecule interactions in aqueous solutions.



1. INTRODUCTION

The effects of salts on protein solubility and conformational stability have been of great research interest for decades. Interestingly, despite their importance in biochemistry, the molecular level mechanism of salt/protein specific interactions is yet to be fully elucidated.¹ There has been a long discussion about how salts can change the properties of proteins, via directly interacting with proteins^{2,3} or indirectly through modifying water structures.^{4,5} It was originally believed that the disruption of water structures by the presence of ions plays a dominant role in biological processes.⁶ However, some recent studies showed that ions only have short-range effects on the structure and dynamics of the first hydration shell but no long-range influence on the water hydrogen bonding network.^{7,8} Recently, the direct ion–biological molecule interactions began to be recognized as a very important factor for the protein stability and solubility.² From X-ray diffraction (XRD) studies on protein structures and molecular dynamics (MD) simulations, anions were found to be able to bind to the positive charged groups of a protein.^{9–13} It was suggested that this direct interaction could be responsible for the solubility of the protein. Because the backbone of a protein is not charged, it was believed that interactions between the amide groups of the backbone and anions were weak and therefore played a very minor role in the salt-induced denaturation.¹⁴ However, an opposite opinion argued that the direct interaction between anions and the amide groups could be responsible for the protein denaturation since the positively charged groups always bind to the anions in both natural and denatured states, resulting in no net contribution to the conformational changes of the proteins.³

The situation that many different opinions on the mechanism of salt/protein interactions coexist partially results from the complexity of the systems investigated. A protein has many functional groups that can potentially interact with ions in aqueous solutions. In a protein solution, these interactions can simultaneously exist, leading to experimental difficulties in determining which interactions are more important than others for changing the conformation of the protein. Instead of studying proteins directly, in this work we have investigated model compounds representing different building blocks of a protein to avoid the copresence of many interactions in one measurement. One model compound represents one functional group which can potentially bind to SCN^- , a strong denaturant. We measured the relative strength of interactions between these model compounds and SCN^- using vibrational energy exchange methods.^{15,16} From these measurements, we were able to determine the relative priorities of these model compounds interacting with SCN^- . Our results show that in aqueous solutions, besides the charged amino acids, other molecules representing the neutral functional groups of a protein can also interact with ions with different strengths.

2. EXPERIMENTS

Materials. Unless specified, chemicals were purchased from Sigma–Aldrich and used as received. $\text{KS}^{13}\text{C}^{15}\text{N}$ was purchased from Cambridge Isotope Laboratory. Formamide- ND_2 was obtained by deuterating formamide in methanol- od .

Received: June 28, 2012

Revised: August 2, 2012

Published: September 17, 2012

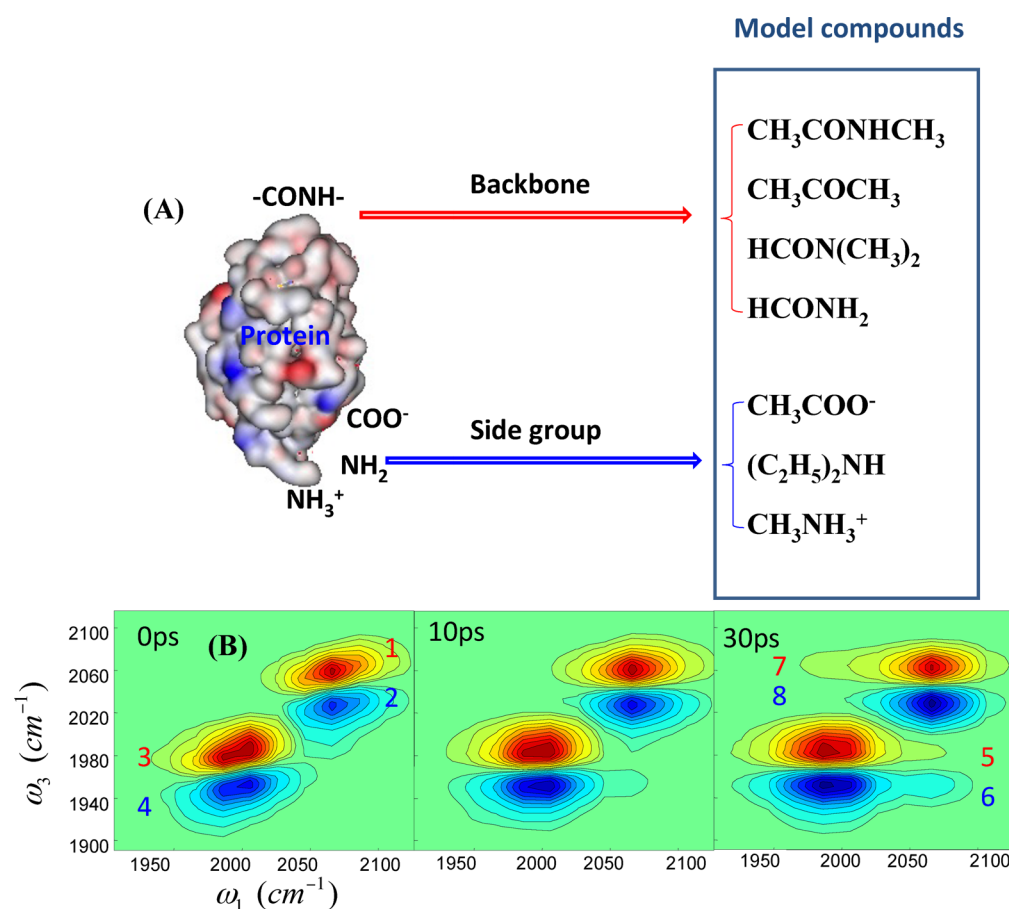


Figure 1. (A) Model compounds of protein building blocks. (B) The time dependence of the 2D IR spectrum of an aqueous solution with Pro:KSCN:KS¹³C¹⁵N:D₂O = 0.4:1:1:20 (molar ratio). As waiting time increases, the off-diagonal peaks (5, 6, 7, 8) grow in because of energy exchange between SCN⁻ and S¹³C¹⁵N⁻.

Methods. The optical setup was described previously.^{15,16} Briefly, a picosecond amplifier and a femtosecond amplifier are synchronized with the same seed pulse from an oscillator which produces ~ 0.6 W 800 nm output with a bandwidth ~ 35 nm and a repetition rate ~ 77 MHz. The picosecond amplifier pumps an OPA to produce ~ 1 ps mid-IR pulses with a bandwidth of $10\text{--}35$ cm^{-1} in a tunable frequency range from 500 to 4000 cm^{-1} with energy $1\text{--}40$ $\mu\text{J}/\text{pulse}$ at 1 kHz. The femtosecond amplifier pumps another OPA to produce 110–150 fs mid-IR pulses with a bandwidth of 200–400 cm^{-1} in a tunable frequency range from 500 to 4000 cm^{-1} with energy $1\text{--}40$ $\mu\text{J}/\text{pulse}$ at 1 kHz. In experiments, the picosecond IR pulse is the pump beam. The femtosecond IR pulse is the probe beam. Its wavelength is measured by a spectrograph, yielding the probe axis (ω_3) of the 2D IR spectrum. Scanning the pump frequency yields the other axis (ω_1) of the spectrum. Two polarizers are inserted into the probe beam path to selectively measure the parallel or perpendicular polarized signal relative to the pump beam. Vibrational lifetimes are obtained from the rotation-free 1–2 transition signal $P_{\text{life}} = P_{\parallel} + 2 \times P_{\perp}$, where P_{\parallel} , P_{\perp} are data from the parallel and perpendicular configurations, respectively. Rotational relaxation times are acquired from the definition $\tau = (P_{\parallel} - P_{\perp}) / (P_{\parallel} + 2 \times P_{\perp})$. Samples were contained in sample cells composed of two CaF₂ windows separated by a plastic spacer. In experiments, the thickness of the spacer was adjusted from 0.5 to 250 μm , depending upon the samples' optical densities. The experimental IR optical path

was purged with clean air free of CO₂ and H₂O. All measurements were carried out at room temperature (22 °C).

3. RESULTS AND DISCUSSION

3.1. Adding Amino Acids into KSCN Aqueous Solutions Can Significantly Slow down the Vibrational Energy Exchange among SCN⁻ Anions. Recently, thiocyanate (SCN⁻) anions were found to be able to form substantial amounts of ion clusters in 1–10 M alkaline metal thiocyanate aqueous solutions.¹⁵ The discovery suggests that in the solutions water molecules and ions tend to separate. The result also implies a relatively weak water/thiocyanate interaction presumably because of the highly delocalized charge on the anion. More experiments on NH₄SCN solutions and mixed salt (KSCN + KF, KI, K₂CO₃, K₂HPO₄, or KOD) further support the ion clustering phenomenon observed and suggest that ion pairing, clustering, and segregations are the results of chemical equilibria among ion/ion, ion/water, and water/water interactions which depends on the chemical nature of the ions.^{17,18} Following the series of experiments, in this work we applied a similar approach to investigate ion/molecule interactions in aqueous solutions by measuring vibrational energy exchanges among isotopically labeled thiocyanate anions.

We utilized the phenomenon that thiocyanate anions in the ion clusters of KSCN aqueous solutions can exchange vibrational energy^{15,16} to determine the relative interaction strength between a model compound and SCN⁻: adding a

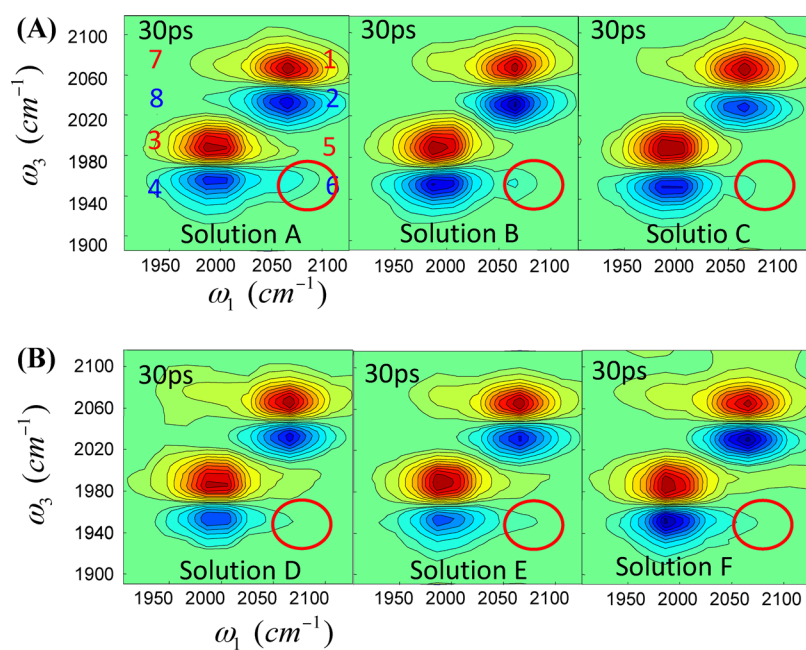


Figure 2. (A) 2D IR spectra at 30 ps of proline-containing solutions compared to KSCN solution without proline. **Solution A** no proline: (KSCN:KS¹³C¹⁵N:D₂O = 1:1:20); **Solution B** (Pro:KSCN:KS¹³C¹⁵N:D₂O = 1:1:1:20); and **Solution C** (Pro:KSCN:KS¹³C¹⁵N:D₂O = 2:1:1:20). (B) 2D IR spectra at 30 ps for solutions containing different amino acids: **Solution D** (Gly:KSCN:KS¹³C¹⁵N:D₂O = 1:1:1:20); **Solution E** (Cys:KSCN:KS¹³C¹⁵N:D₂O = 1:1:1:20); and **Solution F** (Lys:KSCN:KS¹³C¹⁵N:D₂O = 1:1:1:20). Red rings highlight peak 6. The intensity of peak 6 decreases with the addition of all amino acids. The growth of peaks 5 and 7 with the addition of amino acids is caused by the faster vibrational relaxation induced by the direct interactions of the amino acids with the thiocyanate.

model compound into a salt aqueous solution reduces the concentration of water, thus if there is no specific interaction between the ions and the model compound molecules, one would expect that the ion clusters would grow. This will result in a faster observed vibrational energy transfer among the ions as observed in the mixed salt solutions.¹⁸ If the ions interact strongly with the model compound molecules, ions might be removed from the clusters, or the model compound molecules may insert into the ion clusters and increase the average distance among the SCN⁻ anions and also quench the SCN⁻ excitation. This will result in a slower observed vibrational energy transfer among the ions.

The polar functional groups of a typical protein that can potentially interact with ions are the backbone amide groups, the ammonium cations, the carboxylic anions, and the amino acid residues. To determine possible SCN⁻/protein specific interactions, we used different model compounds to represent these different functional groups, as shown in Figure 1A: (1) *N*-methylacetamide (NMA) for the backbone amide groups and acetone for the backbone carbonyl group, (2) carboxylate anion (CH₃COO⁻) for the carboxylic anions, (3) methyl ammonium cation (CH₃NH₃⁺) for the ammonium cations, and (4) glycine (Gly), cysteine (Cys), proline (Pro), and lysine (Lys) for the amino acid residues. In experiments, each of these compounds was added into a 4 M potassium thiocyanate aqueous solution (Solution A: KSCN:KS¹³C¹⁵N:D₂O = 1:1:20 molar ratio). The effective ion cluster concentrations in these samples were then determined by measuring the vibrational energy exchange rates between S¹³C¹⁵N⁻ and SCN⁻ anions.

The vibrational energy exchange method is demonstrated in Figure 1B for an aqueous solution with Pro:KSCN:KS¹³C¹⁵N:D₂O = 0.4:1:1:20 (molar ratio). In the solution, some ions form clusters with each other, and some are separated by other molecules. In the clusters, the thiocyanate

anions can exchange vibrational energy much more efficiently than those separated anions because the energy transfer rate is inversely proportional to the sixth power of the donor/acceptor distance under the general assumption of dipole/dipole interaction.¹⁹ The energy exchange between SCN⁻ and S¹³C¹⁵N⁻ in the clusters produces off-diagonal cross peak pairs (peaks 5 and 6 and 7 and 8) in the 2D IR spectra. At waiting time $T_w = 0$ ps, energy exchange has not occurred. Only two diagonal pairs of peaks show up in the 2D IR spectrum (0 ps panel in Figure 1B). Peak 1 is from the CN stretch 0–1 transition, and peak 2 is from the CN stretch 1–2 transition. Both separated and clustered SCN⁻ anions contribute to these peaks. Peaks 3 and 4 are from the ¹³C¹⁵N stretch 0–1 and 1–2 transitions of S¹³C¹⁵N⁻ anions, respectively. The 1–2 transition peaks are at lower frequencies than their corresponding 0–1 transition peaks because the vibrations are anharmonic. With the increase of the delay time after both anions are vibrationally excited, the vibrational energy begins to exchange between SCN⁻ and S¹³C¹⁵N⁻. The energy exchange induces off-diagonal peak pairs to appear on the off-diagonal positions (10 and 30 ps panels). After a waiting time $T_w = 30$ ps, vibrational energy has exchanged to a substantial degree so that the off-diagonal peak pairs are pronounced. The vibrational energy transfer from SCN⁻ down to S¹³C¹⁵N⁻ produces peaks 5 and 6. The excitation frequency ω_1 of both peaks is 2066 cm⁻¹, which is the CN stretch 0–1 transition frequency, showing that the energy originates from the excitation of the CN stretch of SCN⁻. Their detection frequencies ω_3 are 1993 and 1957 cm⁻¹, which are the ¹³C¹⁵N stretch 0–1 and 1–2 transition frequencies, showing that the energy has been transferred to S¹³C¹⁵N⁻. Similarly, peaks 7 and 8 are from the process of energy transfer from S¹³C¹⁵N⁻ up to SCN⁻. Because the off-diagonal peaks arise mainly from the clustered anions and the diagonal peaks are from both separated and clustered species,

simultaneous analyses on the time evolutions of both diagonal and off-diagonal peaks provide not only the energy exchange rates but also the concentration of the ion clusters. Among the four energy exchange peaks, peaks 5 and 7 also contain significant contributions from the heat effect at long waiting times. Relaxation of vibrational excitation produces heat which creates bleaching at frequencies near the CN and $^{13}\text{C}^{15}\text{N}$ stretch 0–1 transition frequencies, as manifested by the temperature difference FTIR spectra shown in Figure S15 in the Supporting Information.^{20,21} The temperature difference FTIR spectra also show that the heat effect at the 1–2 transition frequencies is much smaller. Therefore, peaks 6 and 8 are more suitable than peaks 5 and 7 for analyzing the mode-specific energy transfer kinetics. However, peak 8 slightly overlaps with peak 3. Thus, the intensity of peak 6 is the most straightforward signal for comparing energy transfer rates in different samples. A bigger normalized intensity of peak 6 at the same delay time represents a faster apparent energy transfer rate.

Figure 2A displays 2D IR spectra of potassium thiocyanate aqueous solutions with the additions of different amounts of proline: **Solution A** (without amino acids) ($\text{KSCN}:\text{K}^{13}\text{C}^{15}\text{N}:\text{D}_2\text{O} = 1:1:20$); **Solution B** ($\text{Pro}:\text{KSCN}:\text{K}^{13}\text{C}^{15}\text{N}:\text{D}_2\text{O} = 1:1:1:20$); and **Solution C** ($\text{Pro}:\text{KSCN}:\text{K}^{13}\text{C}^{15}\text{N}:\text{D}_2\text{O} = 2:1:1:20$). With the increase of proline concentration from 0 (**Solution A**) to 4 M (**Solution C**), the intensity of peak 6 gradually drops $\sim 50\%$. As discussed before,¹⁵ peaks 5–8 are mainly from vibrational energy exchange between SCN^- and $\text{S}^{13}\text{C}^{15}\text{N}^-$ at relatively short waiting times. Faster energy transfers produce larger cross peaks at the same waiting time. At longer times, heat effects grow in, which can affect peaks 5, 7, and 8. Peak 6 is hardly affected by heat because of its lower detection frequency as described in the previous paragraph.^{20,21} A simple inspection of the intensity of peak 6 reveals that the vibrational energy exchange between SCN^- and $\text{S}^{13}\text{C}^{15}\text{N}^-$ slows down by $\sim 50\%$ with the addition of 4 M proline. The R-NH_3^+ cations of proline are expected to bind to SCN^- , similar to the binding of NH_4^+ cations to the anions in concentrated NH_4SCN aqueous solutions.¹⁷ The binding can lead to a larger average distance among the SCN^- anions by either inserting proline into the clusters or removing SCN^- out of the clusters. The binding can also quench the CN excitation. These factors can slow down the observed energy transfer rates among the anions.

In addition, adding 4 M proline to the 4 M potassium thiocyanate solution can change the transition dipole moment of the CN or $^{13}\text{C}^{15}\text{N}$ stretch and the refractive index of the solution. These two factors can also affect the vibrational energy transfer rates. We measured and calculated the changes of the transition dipole moments and refractive indexes and found that the effects of these two changes on the concentration of energy-transferable SCN^- anions are actually small for all samples studied in this work. Measurements and corrections on the transition dipole moment and refractive index changes are provided in the Supporting Information.

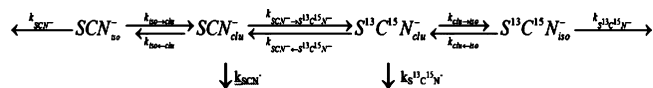
The slowdowns of energy transfer observed in **Solutions B–C** are not exceptions. Adding 2 M glycine, 2 M cysteine, or 2 M lysine into **Solution A** has a similar effect (Figure 2B). The intensity of the vibrational energy transfer peak 6 decreases dramatically in each case, indicating a slower energy transfer. In contrast, the intensity of peak 7 increases with the addition of amino acids. Similar to those thoroughly analyzed for other systems,^{20–22} the intensity increase of peak 7 is mainly a result

of the heat effect from the faster vibrational relaxation of the thiocyanate anions induced by the interactions with amino acids. As experimentally measured, the vibrational relaxation time of the CN stretch first excited state drops from ~ 30 ps in the 4 M $\text{KSCN}/\text{K}^{13}\text{C}^{15}\text{N}/\text{D}_2\text{O}$ solution (solution A) to ~ 15 ps with the addition of 4 M proline (solution C). Adding other amino acids has similar effects. Vibrational lifetimes of all samples are included in the Supporting Information under “kinetic model and fitting results”. The introduction of OH groups from the H/D exchange between the amino acids and D_2O can also slightly reduce the vibrational lifetimes of thiocyanate anions but to a much lesser extent. However, this can be simulated by adding H_2O , and no heat effect is observed from such an H/D exchange. Data are in the Supporting Information.

3.2. Addition of Amino Acids Reduces Ion Clustering.

To quantitatively analyze the vibrational energy exchange kinetics with the additions of amino acids, we constructed a kinetic model based on our previous work.¹⁵ In the model, the net effects of model compounds binding to thiocyanate were considered to reduce the concentration of thiocyanate anions which can effectively transfer energy to other anions. We named these energy-transferable anions as “clustered” ions. The thiocyanate anions in solution can be simply divided into two components: thiocyanate anions bound to model compounds or water molecules that cannot exchange vibrational energy and therefore are called “isolated” and “clustered” thiocyanate anions that can exchange vibrational energy. All of the thiocyanate anions contribute to the diagonal peak pairs in 2D IR measurements, but only the clustered anions contribute to the off-diagonal peak pairs. The vibrational excitations of the anions decay with their own lifetimes. The observed changes of energy exchange rates are caused by the concentration change of clustered ions. In the model, we assume that once a thiocyanate anion is bound to a model compound it will not be able to exchange energy with other anions because the energy from this bound anion will probably transfer to the model compounds. The shortened CN lifetimes with the additions of amino acids into **Solution A** support this assumption (in the Supporting Information). At room temperature, the clustered ions and the isolated ions are under dynamic equilibrium. The kinetic model can be illustrated in Scheme 1.

Scheme 1



From the model, four differential equations are derived as below

$$\begin{aligned} \frac{d[\text{SCN}^-_{\text{clu}}(t)^*]}{dt} &= k_{\text{iso} \rightarrow \text{clu}}[\text{SCN}^-_{\text{iso}}(t)^*] \\ &\quad + k_{\text{SCN}^- \leftarrow \text{S}^{13}\text{C}^{15}\text{N}^-}[\text{S}^{13}\text{C}^{15}\text{N}^-_{\text{clu}}(t)^*] \\ &\quad - (k_{\text{iso} \leftarrow \text{clu}} + k_{\text{SCN}^- \rightarrow \text{S}^{13}\text{C}^{15}\text{N}^-} + k_{\text{SCN}^-}) \\ &\quad [\text{SCN}^-_{\text{clu}}(t)^*] \quad (1) \end{aligned}$$

$$\begin{aligned} \frac{d[\text{SCN}^-_{\text{iso}}(t)^*]}{dt} &= k_{\text{iso} \leftarrow \text{clu}}[\text{SCN}^-_{\text{clu}}(t)^*] \\ &\quad - (k_{\text{SCN}^-} + k_{\text{iso} \rightarrow \text{clu}})[\text{SCN}^-_{\text{iso}}(t)^*] \quad (2) \end{aligned}$$

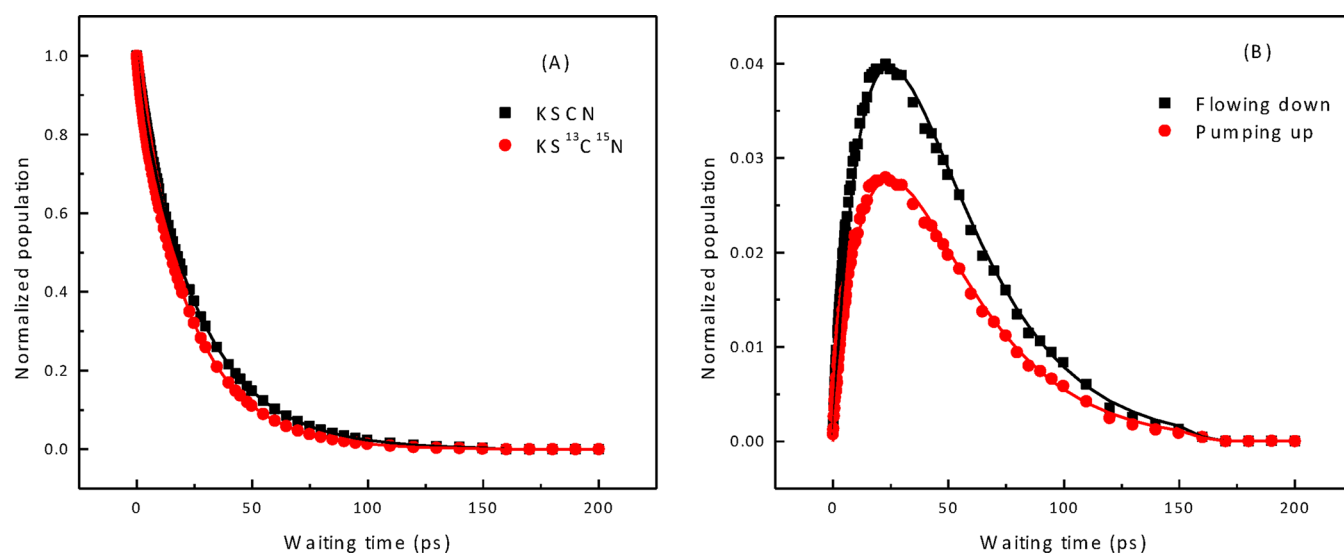


Figure 3. Data and calculations of **Solution A** (4.0 M KSCN/ $\text{KS}^{13}\text{C}^{15}\text{N}$ D_2O solution). Dots are data, and lines are calculations.

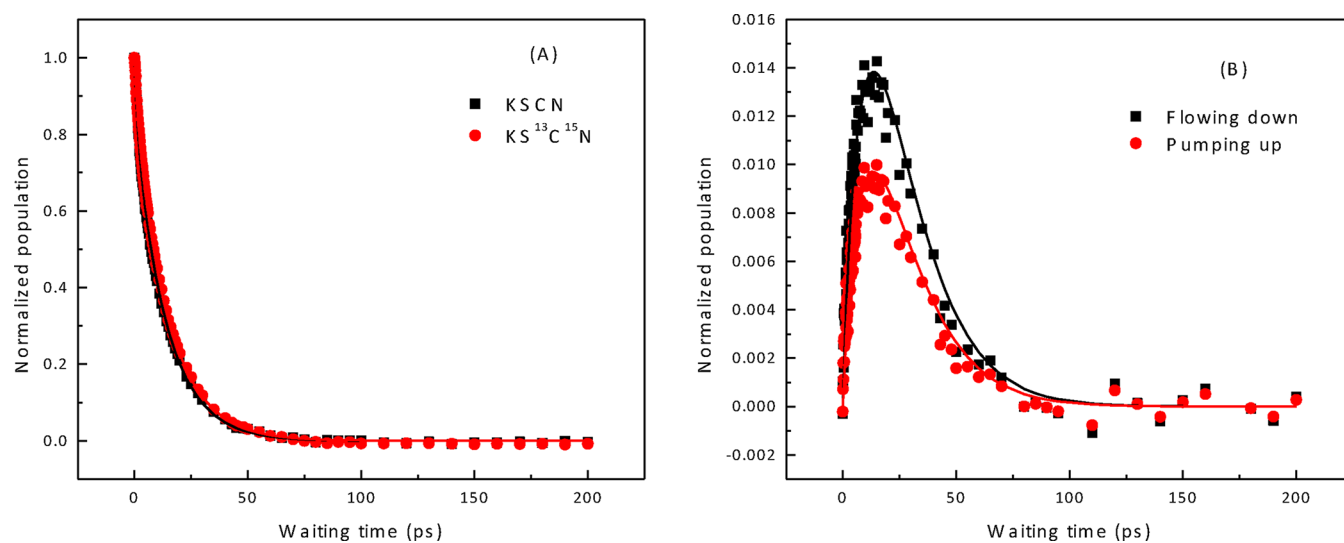


Figure 4. Data and calculations of **Solution B** (Pro:KSCN: $\text{KS}^{13}\text{C}^{15}\text{N}$: D_2O = 1:1:1:20). Dots are data, and lines are calculations.

$$\begin{aligned} \frac{d[\text{S}^{13}\text{C}^{15}\text{N}_{\text{clu}}^-(t)^*]}{dt} &= k_{\text{iso} \rightarrow \text{clu}}[\text{S}^{13}\text{C}^{15}\text{N}_{\text{iso}}^-(t)^*] + k_{\text{SCN}^- \rightarrow \text{S}^{13}\text{C}^{15}\text{N}^-}[\text{SCN}_{\text{clu}}^-(t)^*] \\ &\quad - (k_{\text{iso} \rightarrow \text{clu}} + k_{\text{SCN}^- \leftarrow \text{S}^{13}\text{C}^{15}\text{N}^-} k_{\text{S}^{13}\text{C}^{15}\text{N}^-})[\text{S}^{13}\text{C}^{15}\text{N}_{\text{clu}}^-(t)^*] \end{aligned} \quad (3)$$

$$\begin{aligned} \frac{d[\text{S}^{13}\text{C}^{15}\text{N}_{\text{iso}}^-(t)^*]}{dt} &= k_{\text{iso} \leftarrow \text{clu}}[\text{S}^{13}\text{C}^{15}\text{N}_{\text{clu}}^-(t)^*] - (k_{\text{S}^{13}\text{C}^{15}\text{N}^-} + k_{\text{iso} \rightarrow \text{clu}}) \\ &\quad [\text{S}^{13}\text{C}^{15}\text{N}_{\text{iso}}^-(t)^*] \end{aligned} \quad (4)$$

The time-dependent populations (isolated SCN^- , clustering SCN^- , isolated $\text{S}^{13}\text{C}^{15}\text{N}^-$, and clustering $\text{S}^{13}\text{C}^{15}\text{N}^-$) and vibrational lifetimes are experimentally determined. The isolated and clustered species equilibrium constant K ($K = (k_{\text{iso} \rightarrow \text{clu}})/(k_{\text{iso} \leftarrow \text{clu}})$) determines the location exchange rate constant ratio. The energy exchange rate constant ratio D is determined by the energy mismatch of the two vibrations. The normalized initial populations are: $[\text{SCN}_{\text{clu}}^-(0)^*] = (K)/(K +$

$1)$, $[\text{SCN}_{\text{iso}}^-(0)^*] = (1)/(K + 1)$, $[\text{S}^{13}\text{C}^{15}\text{N}_{\text{clu}}^-(0)^*] = [\text{S}^{13}\text{C}^{15}\text{N}_{\text{iso}}^-(0)^*] = 0$. Solving equations (eq 1 ~ eq 4) with experiment results gives the energy transfer rate constants, the isolated-clustered ion exchange rate constants ($k_{\text{iso} \rightarrow \text{clu}}$ and $k_{\text{iso} \leftarrow \text{clu}}$), and the isolated/clustered equilibrium constant (K).

For the solutions, the energy mismatch between the CN and $^{13}\text{C}^{15}\text{N}$ stretches is 73 cm^{-1} , determining that $D = (k_{\text{S}^{13}\text{C}^{15}\text{N}^- \rightarrow \text{SCN}^-})/(k_{\text{SCN}^- \rightarrow \text{S}^{13}\text{C}^{15}\text{N}^-}) = 0.7$. Our previous experiments¹⁵ show that from 4 M KSCN aqueous solution to 1.8 M solution the cluster percentage decreases from 67% to 35%. However, the average cluster size remains almost constant (the number of anions in a cluster changes from 5 to 4). In solutions A~O, the cluster percentage is within this range. Therefore, we assume that the cluster size is constant in all solutions so that we can use the same energy transfer rate constant for all samples in the calculations to have a fair comparison for the cluster percentage in different samples.

Analyses based on experimental results and the kinetic model for solution A give $k_{\text{SCN}^- \rightarrow \text{S}^{13}\text{C}^{15}\text{N}^-} = 1/140 \text{ (ps}^{-1}\text{)}$. The equilibrium constant, K , is 2.0, indicating that the cluster percentage is 67%. The location exchange rate constant is $(1/$

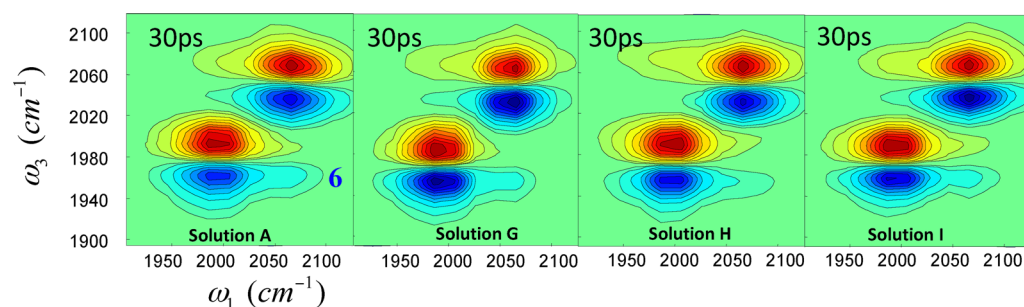


Figure 5. Chemical dependence of 2D IR spectra of solutions at 30 ps: **Solution A** (KSCN:KS¹³C¹⁵N:D₂O = 1:1:20); **Solution G** (CH₃COOK:KSCN:KS¹³C¹⁵N:D₂O = 2:1:1:20); **Solution H** (CH₃NH₃Cl:KSCN:KS¹³C¹⁵N:D₂O = 1:1:1:20); **Solution I** (KCl:KSCN:KS¹³C¹⁵N:D₂O = 0.9:1:1:20).

$k_{\text{clu} \rightarrow \text{iso}} = 15 \pm 7$ (ps⁻¹). Experimental results and calculations based on the kinetic model with the following parameters are displayed in Figure 3

$$\begin{aligned} k_{\text{SCN}^- \text{fast}} &= 1/3.1 \text{ (ps}^{-1}\text{)}; k_{\text{SCN}^- \text{slow}} \\ &= 1/30.5 \text{ (ps}^{-1}\text{)}; k_{\text{S}^{13}\text{C}^{15}\text{N}^- \text{fast}} \\ &= 1/2.1 \text{ (ps}^{-1}\text{)}; k_{\text{S}^{13}\text{C}^{15}\text{N}^- \text{slow}} \\ &= 1/25.1 \text{ (ps}^{-1}\text{)}; k_{\text{clu} \rightarrow \text{iso}} \\ &= 1/10 \text{ (ps}^{-1}\text{)}; K \\ &= 2.0; k_{\text{SCN}^- \rightarrow \text{S}^{13}\text{C}^{15}\text{N}^-} \\ &= 1/140 \text{ (ps}^{-1}\text{)}; D \\ &= 0.7 \end{aligned}$$

with prefactors of the subgroups and offset of the biexponential

$$\begin{aligned} A_{\text{SCN}^- \text{fast}} &= 0.05; A_{\text{SCN}^- \text{slow}} \\ &= 0.95; A_{\text{S}^{13}\text{C}^{15}\text{N}^- \text{fast}} \\ &= 0.07; A_{\text{S}^{13}\text{C}^{15}\text{N}^- \text{slow}} \\ &= 0.93; \text{offset} \\ &= 0 \end{aligned}$$

With the addition of 2 M proline (**Solution B**), as we can see from Figure 2A, the vibrational energy exchanges among SCN⁻ anions slow down. Quantitative analyses based on the above model show that the concentration of clustered ions is 48%. Calculations and experimental results are displayed in Figure 4. The calculation parameters are

$$\begin{aligned} k_{\text{SCN}^- \text{fast}} &= 1/1.5 \text{ (ps}^{-1}\text{)}; k_{\text{SCN}^- \text{slow}} \\ &= 1/14.5 \text{ (ps}^{-1}\text{)}; k_{\text{S}^{13}\text{C}^{15}\text{N}^- \text{fast}} \\ &= 1/1.1 \text{ (ps}^{-1}\text{)}; k_{\text{S}^{13}\text{C}^{15}\text{N}^- \text{slow}} \\ &= 1/15.0 \text{ (ps}^{-1}\text{)}; k_{\text{clu} \rightarrow \text{iso}} \\ &= 1/10 \text{ (ps}^{-1}\text{)}; K \\ &= 0.92; k_{\text{SCN}^- \rightarrow \text{S}^{13}\text{C}^{15}\text{N}^-} \\ &= 1/140 \text{ (ps}^{-1}\text{)}; D \\ &= 0.7 \end{aligned}$$

with prefactors of the subgroups and offset of the single-exponential

$$\begin{aligned} A_{\text{SCN}^- \text{fast}} &= 0.15; A_{\text{SCN}^- \text{slow}} \\ &= 0.85; A_{\text{S}^{13}\text{C}^{15}\text{N}^- \text{fast}} \\ &= 0.10; A_{\text{S}^{13}\text{C}^{15}\text{N}^- \text{slow}} \\ &= 0.90; \text{offset} \\ &= 0 \end{aligned}$$

Analyses and experimental results of all other samples that were examined in this work are provided in the Supporting Information.

3.3. K⁺/Carboxylate Anion Interaction Is Not Responsible for the Slower Energy Transfer Observed. Now, the next issue to explore is which specific interaction is responsible for the observed slower energy transfer with the addition of amino acids: the thiocyanate/ammonium interaction or the K⁺/carboxylate anion interaction. This topic was investigated by measuring the vibrational energy transfers among thiocyanate anions in solutions with the addition of CH₃COOK or CH₃NH₃Cl. 2D IR spectra at 30 ps of solutions with the addition of CH₃COOK (**Solution G**, CH₃COOK:KSCN:KS¹³C¹⁵N:D₂O = 2:1:1:20) and CH₃NH₃Cl (**Solution H**, CH₃NH₃Cl:KSCN:KS¹³C¹⁵N:D₂O = 1:1:1:20) are displayed in Figure 5. With the addition of 4 M CH₃COO⁻K⁺, the intensity of peak 6 has almost no change (panel **Solution G**) compared to without the addition (panel **Solution A**), implying that the interaction between K⁺ and the carboxylate anion (if any) plays a very minor role in disrupting the concentration of ion clusters in the amino acid solutions B~F. In contrast, the addition of only ~2 M of CH₃NH₃⁺Cl⁻ produces a substantial change in the intensity of peak 6 (panel **Solution H**). The change can be caused either by the binding between the ammonium cation and the thiocyanate anion or by the interaction between Cl⁻ and K⁺ inside the clusters. The latter possibility is excluded by experiments. As shown in panel **Solution I**, when ~1.8 M KCl was added into **Solution A**, no obvious change in the intensity of peak 6 was observed. The series of experiments reveals that the ammonium cation does interact with the thiocyanate anion. The observations agree with our recent experiments that NH₄⁺ can directly bind to SCN⁻ in aqueous solutions.¹⁷ They also agree with the recent theoretical finding that the strong "chaotropic" ammonium group of amino acids can form direct ion pairs with strong "chaotropic" anions.^{23,24} Quantitative analyses based on the kinetic model described above show that the addition of 2 M CH₃NH₃⁺Cl⁻ reduces the concentration of clustered ions to ~44% from 67% in solution A. H⁺ from possible deprotonation of the amino acids is not a likely reason for the observed slowed

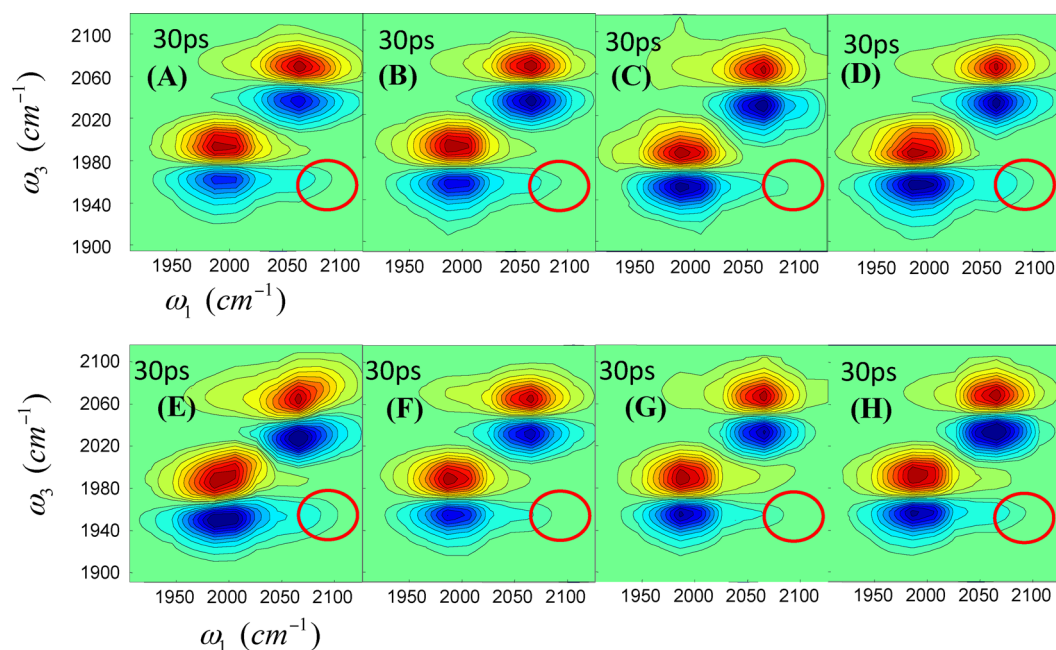


Figure 6. 2D IR spectra at 30 ps of (A) **Solution A** (KSCN:KS¹³C¹⁵N:D₂O = 1:1:20); (B) **Solution J** (NMA:KSCN:KS¹³C¹⁵N:D₂O = 2:1:1:20); (C) **Solution K** (NMA:KSCN:KS¹³C¹⁵N:D₂O = 4:1:1:20); (D) **Solution L** (Acetone:KSCN:KS¹³C¹⁵N:D₂O = 2:1:1:20); (E) **Solution M** (DMF:KSCN:KS¹³C¹⁵N:D₂O = 2:1:1:20); (F) **Solution N** (HCONH₂:KSCN:KS¹³C¹⁵N:D₂O = 2:1:1:20); (G) **Solution O** ((C₂H₅)₂NH:KSCN:KS¹³C¹⁵N:D₂O = 2:1:1:20); and (H) **Solution P** ((C₂H₅)₃N:KSCN:KS¹³C¹⁵N:D₂O = 2:1:1:20).

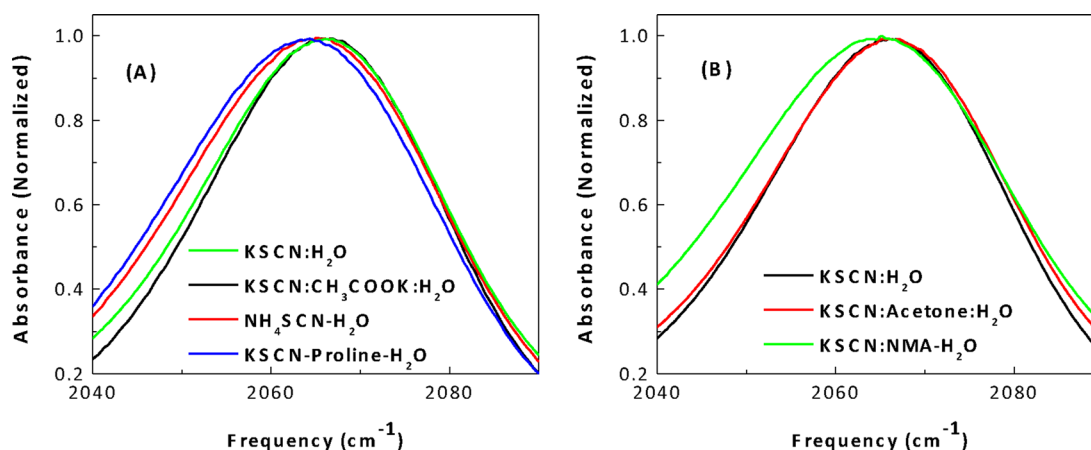


Figure 7. FTIR spectra of (A) KSCN:CH₃COOK:H₂O = 1:1:10 (black line); NH₄SCN:H₂O = 1:10 (red line); KSCN:H₂O = 1:10 (green line); KSCN:proline:H₂O = 1:1:10 (blue line); (B) KSCN:H₂O = 1:10 (black line); KSCN:acetone:H₂O = 1:1:10 (red line); KSCN:NMA:H₂O = 1:1:10 (green line).

energy transfer because the pH values of the solutions are close to or higher than 7 as measured. The concentration of H⁺ is too small compared to that of RNH₃⁺ or K⁺ to have any important effect on the ion clustering.

3.4. N–H Group in the Backbone Can Also Slow Down the Vibrational Energy Transfer.

We used a similar strategy to investigate the salt/amide backbone interactions. As displayed in Figure 6B and C, adding 4 M NMA (*N*-methylacetamide) into **Solution A** slightly slows down the vibrational energy exchange. NMA has three possible sites

binding to thiocyanate: the carbonyl group () , the amide bond () , and the N–H group () . We used acetone to represent the carbonyl group. As shown in Figure 6D, adding 4 M acetone into **Solution A** produces a negligible

change in the vibrational energy transfer rate among the thiocyanate anions, implying that the interactions between the carbonyl group and the ions are very weak. Adding 4 M DMF (HCON(CH₃)₂, Figure 6E) has a similar but very slight effect. However, adding 4 M formamide (HCONH₂, FMA, Figure 6F) into **Solution A** produces a clear decrease in the intensity of peak 6, indicating a stronger interaction between the ions and formamide. Formamide has two more N–H's than DMF (note, the two N–H's are slightly different because of their different locations) and one more N–H than NMA. The results in Figure 6B,E, and F imply that the N–H group plays an important role for the amide group binding to the ions (the quantitative analysis on DMF shows that the amide bond also plays a role, see Supporting Information). Because formamide is less electron-rich than the other two molecules, the ions bound to its N–H's are probably the thiocyanate anions (to H)

Table 1. Relative Binding Affinities of Model Compounds with the Thiocyanate Anion

solution	B (Pro)	D (Gly)	E (Cys)	F (Lys)	G (CH ₃ COOK ⁻)	H (CH ₃ NH ₃ ⁺)	J (NMA)	L (acetone)	M (DMF)	N (FMA)	O (DEA)
<i>K</i> _{Affinity}	19 ± 8	25 ± 10	53 ± 19	70 ± 5.5	1.4 ± 1	25 ± 10	2.7 ± 2	1.4 ± 1	2.7 ± 2	5 ± 2.5	5 ± 2

rather than the K⁺ cations (to the lone electron pair). The conclusions are supported by further experiments. Adding 4 M diethylamine ((C₂H₅)₂NH, DEA) into **Solution A**, which clearly reduces the intensity of peak 6 (Figure 6G), indicates a strong interaction between the amine group and the ions, while adding 4 M triethylamine ((C₂H₅)₃N) to **Solution A** does not change the intensity of peak 6 (Figure 6H) as much, indicating the insignificance of the interaction between the lone electron pair and K⁺. The results also explain why the effect of lysine is bigger than proline (Figure 2B), probably because lysine has an extra amine group which is able to bind to thiocyanate. It is interesting to note that in solutions with amino acids (proline), NH₄⁺, and NMA the CN stretch 0–1 transition central frequency red shifts for about 2 cm⁻¹, compared to that in the 4 M KSCN solution. In contrast, adding 4 M CH₃COOK or acetone does not cause such a frequency shift, as displayed in Figure 7. The results show that the molecules with the positively charged groups or the amide groups probably have a bigger effect on the CN vibration of SCN⁻ than the molecules without them in aqueous solutions.

Quantitative analyses show that the concentration of clustered anions is slightly reduced to 58% ± 4% from 67% with the addition of 4 M NMA, to 52% ± 4% with the addition of 4 M FMA, and to 62% ± 4% with the addition of 4 M acetone.

3.5. Binding Affinity of SCN⁻ and Charged Amino Acid Residues Is About 20 Times Bigger than That between the Water Molecules and the Amino Acids. The simple inspections on the vibrational energy exchange 2D IR spectra have provided us a qualitative picture about the relative binding strength of different model compounds with thiocyanate in aqueous solutions. To quantitatively describe the relative binding affinity of the model compounds to the thiocyanate anions, we constructed an equilibrium model consistent with the kinetic model to analyze the vibrational energy exchange results. Using **Solution C** as an example, three types of thiocyanate anions coexist under chemical equilibrium: clustered (SCN⁻_{clustered}), hydrated (SCN⁻_{hydrated}), and proline-complexed (SCN⁻_{pro}). Two types of proline molecules coexist: hydrated (pro_{hydrated}, including the self-associated proline) and thiocyanate-complexed (pro_{SCN⁻}). The binding affinity between thiocyanate and proline is defined as

$$K_{\text{affinity}} = \frac{[\text{SCN}_{\text{pro}}^-][\text{D}_2\text{O}]^n}{[\text{SCN}_{\text{hydrated}}^-][\text{pro}_{\text{hydrated}}]} \quad (5)$$

from the following equilibrium



In the model, we assumed that the extent of self-association of proline is small because of the relatively big amounts of water and KSCN. The total concentration of water was taken as constant since the amount of additive is relatively small, leading to a constant concentration of hydrated thiocyanate anions. In this approximation, proline/thiocyanate complexes in both water and ion clusters are mathematically combined into one parameter: SCN⁻_{pro}. The concentration sum of proline-complexed and hydrated thiocyanate anions was obtained

from the vibrational energy exchange experiments, and the concentration of proline was known beforehand. Equation 5 is readily solvable with all these parameters known. The number of water molecules in eq 5 was set to be 1 for comparison of the one-to-one binding affinity. On the basis of this model and the vibrational energy exchange results, the relative affinity (compared to water) of proline with thiocyanate was determined to be 19 ± 8. This result is also consistent with the potassium thiocyanate concentration-dependent energy exchange measurements: in the 4 M potassium thiocyanate aqueous solution (**Solution A**, salt:D₂O = 1:10), 33% of the thiocyanate anions are not clustered, and the number is 65% in a 1.8 M solution (salt:D₂O = 1:25).¹⁵ In **Solution C** (proline:salt:D₂O = 1:1:10), 66% of the thiocyanate anions are not clustered. Comparing **Solution C** and the 1.8 M solution, the effect of one proline binding to thiocyanate is roughly equal to that of 15 water molecules in the aqueous solutions. The relative affinity values of other model compounds with thiocyanate were also determined in a similar manner, listed in Table 1. Data in Table 1 show that the affinity of the ammonium cation of amino acids with thiocyanate is only 5–20 times bigger than that of the amide group.

The series of experiments also demonstrates that the chemical natures of the ions and molecules play critical roles in the specific ion/molecule interactions in aqueous solutions. The macroscopic dielectric constants of the molecules are minor factors. For example, the dielectric constant of acetone is ~22, and that of diethylamine is ~4, but the binding affinity of diethyl amine to thiocyanate is obviously stronger than that between acetone and the anion.

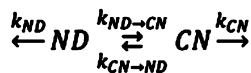
3.6. Direct Energy Transfer from the ND Stretches of Formamide-ND₂ to the CN Stretch of SCN⁻. The hydrogen bond between the amine bond (N–D) of the amide group and SCN⁻ was also investigated by directly measuring the energy transfer from the ND stretch (2400 cm⁻¹) of the amide group to the CN stretch (2060 cm⁻¹) of SCN⁻ in a KSCN/formamide-ND₂ (1/5 molar ratio, HCOND₂) solution. The N–D stretch frequency is around 2400 cm⁻¹, and the CN stretch central frequency is 2065 cm⁻¹. The two vibrational modes can exchange vibrational energy with each other, and the excitations of the two modes can decay with their own lifetimes. On the basis of the physical picture, a previously constructed kinetic model (Scheme 2) was used to analyze the energy transfer kinetics

$$\frac{d[\text{ND}(t)^*]}{dt} = [\text{CN}(t)^*]k_{\text{CN} \rightarrow \text{ND}} - [\text{ND}(t)^*]k_{\text{ND}} - [\text{ND}(t)^*]k_{\text{ND} \rightarrow \text{CN}} \quad (7)$$

$$\frac{d[\text{CN}(t)^*]}{dt} = [\text{ND}(t)^*]k_{\text{ND} \rightarrow \text{CN}} - [\text{CN}(t)^*]k_{\text{CN}} - [\text{CN}(t)^*]k_{\text{CN} \rightarrow \text{ND}} \quad (8)$$

The time dependent populations (CN and ND) and vibrational lifetimes are experimentally determined. The energy exchange rate constant ratio $D = (k_{\text{CN} \rightarrow \text{ND}})/(k_{\text{ND} \rightarrow \text{CN}})$ is determined by the energy mismatch of the two vibrations: $D = 0.2$. Solving equations eq 7 and eq 8 with experiment data gives

Scheme 2



the energy transfer rate constant $k_{CN \rightarrow ND} = 1/8 \text{ ps}^{-1}$. The experimental and calculation results are displayed in Figure 8. The parameters in calculations are

$$\begin{aligned} k_{ND}^- &= 2.0; k_{SCN}^- \text{fast} \\ &= 1/2.26 \text{ (ps}^{-1}\text{)}; k_{SCN}^- \text{slow} \\ &= 1/21.50 \text{ (ps}^{-1}\text{)}; k_{ND^- \rightarrow CN^-} \\ &= 1/8.0 \text{ (ps}^{-1}\text{)}; D \\ &= 0.2 \end{aligned}$$

with prefactors of the subgroups and offset of the biexponential

$$A_{SCN^- \text{fast}} = 0.16; A_{SCN^- \text{slow}} = 0.84; \text{offset} = 0$$

Using the same procedure, analyses show that the energy transfers from OD to CN in the KSCN/D₂O = 1:5 solution with a rate constant $K_{OD \rightarrow CN} = (1/17) \text{ ps}^{-1}$. Parameters used in calculations are $k_{CN} = (1/70.0) \text{ ps}^{-1}$; $k_{OD} = 1.0 \text{ ps}^{-1}$. Similar to the NH₄SCN experiments,¹⁷ the measured ND/CN and OD/CN energy transfers also have some contributions from bridged pathways through some combination bands.

The above kinetic analysis shows that the energy transfer ND (2400 cm⁻¹) → CN (2060 cm⁻¹) time constant is $(1/k_{ND \rightarrow CN}) = 8 \pm 1 \text{ ps}$. Experiments also show that the OD (2400 cm⁻¹) → CN (2066 cm⁻¹) transfer time constant in a KSCN/D₂O (1:5 molar ratio) is $(1/k_{OD \rightarrow CN}) = 17 \pm 1 \text{ ps}$. Normalized with the differences $((\mu_{ND}^2)/(\mu_{OD}^2) = 1.2)$ of transition dipole moment and refractive index and the transition dipole cross angles from

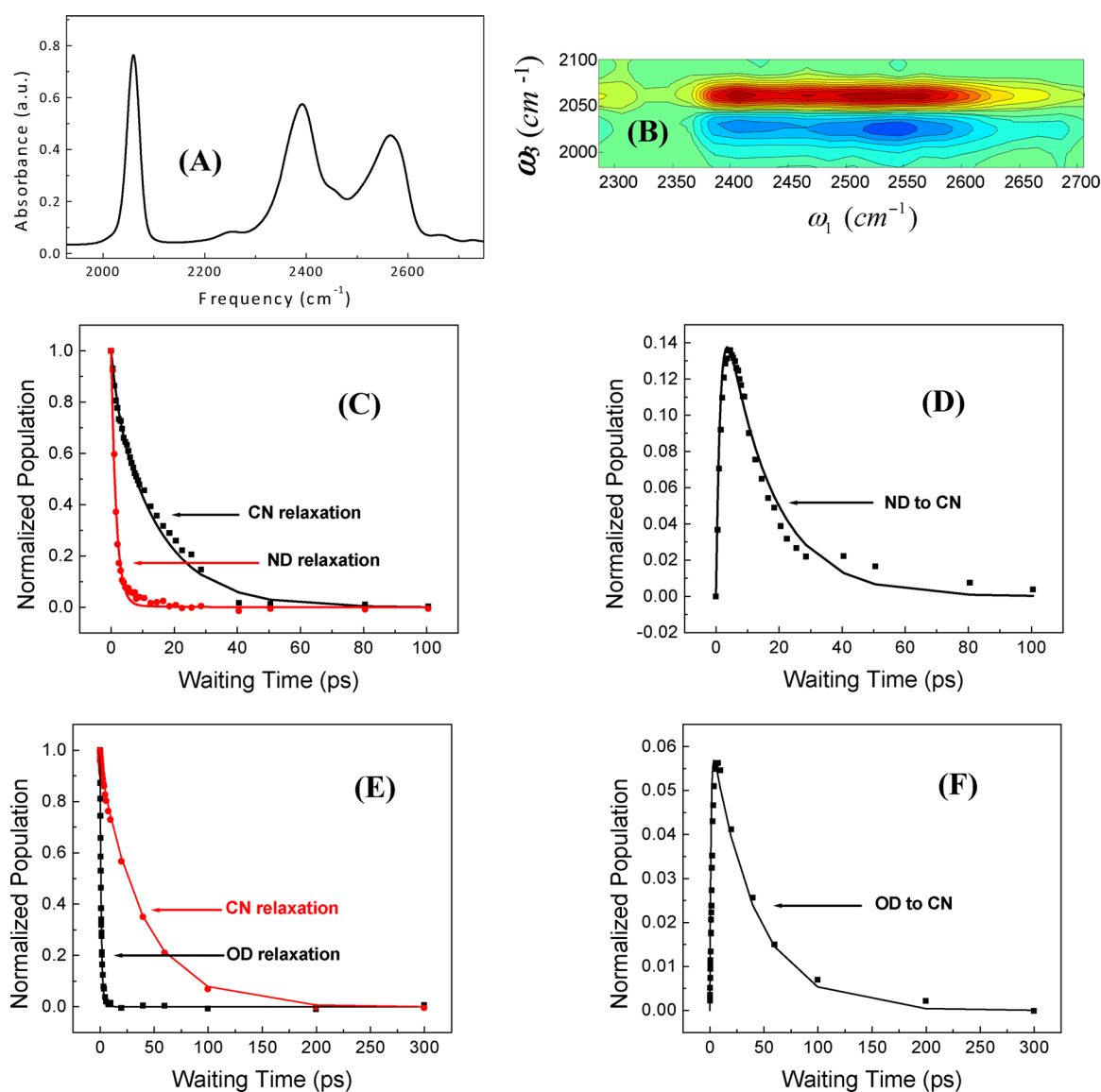


Figure 8. (A) FTIR spectrum of a formamide-ND₂/KSCN = 5:1 solution. ND stretches have one peak at $\sim 2400 \text{ cm}^{-1}$ and another at 2560 cm^{-1} . (B) 2D IR spectrum at 5 ps of the solution showing the energy transfer cross peaks from the ND stretches to the CN stretches. (C) and (F) are experimental data (dots) and kinetic calculations (lines) for the ND stretch (2400 cm^{-1}) relaxation, the CN stretch relaxation (2060 cm^{-1}), the ND to CN energy transfer, the OD stretch (2400 cm^{-1}) relaxation, the CN stretch relaxation (2066 cm^{-1}), and the OD to CN energy transfer in the a formamide-ND₂/KSCN = 5:1 solution and a D₂O/KSCN = 5:1 solution.

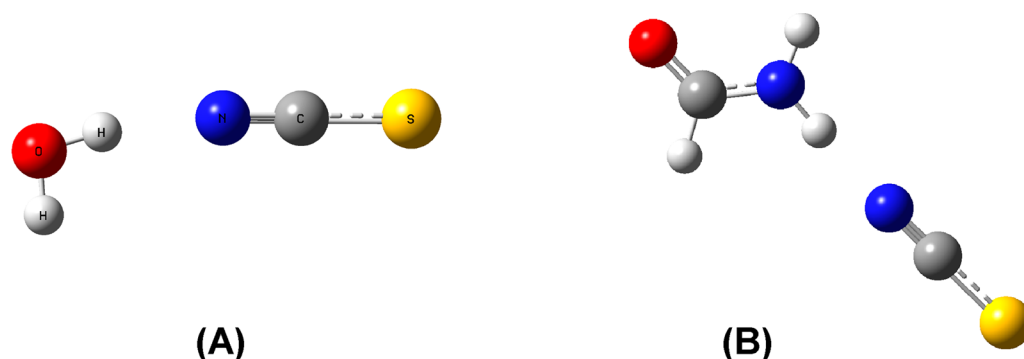


Figure 9. Structures of (A) $\text{H}_2\text{O}/\text{SCN}^-$ and (B) formamide/ SCN^- dimers from DFT calculations for gas phase molecules. The basis set is 6-311++G(d,p).

calculations, the energy transfer rate ratio $(k_{\text{ND} \rightarrow \text{CN}})/(k_{\text{OD} \rightarrow \text{CN}})$ is 1.7. According to the dipole/dipole approximation, the normalized larger ND to CN energy transfer rate implies a shorter or at least comparable distance of ND/CN, compared to that of OD/CN. As mentioned above, we found that part of the energy can transfer in both systems through combination bands. The energy transfer mechanism through combination bands is not necessary in the dipole/dipole interaction, which is to be explored in our future work. Therefore, the energy transfer rate ratio reported here can not be immediately translated into the donor/acceptor distance ratio based on the dipole/dipole interaction. Nonetheless, the energy transfer measurements show that the SCN^- anions can stay close to the NH groups of formamide. These results are consistent with the above ion clustering measurements. Calculated $\text{H}_2\text{O}/\text{SCN}^-$ and formamide/ SCN^- dimer structures are displayed in Figure 9.

4. CONCLUDING REMARKS

As demonstrated in this work, interactions between SCN^- and some amino acids, the amide group, and the amine group of some organic compounds in aqueous solutions were observed. Quantitative analyses show that the interaction strength between SCN^- and the charged amino acid residues is about 20 times bigger than that between the water molecules and the amino acids and about 5–10 times larger than that between SCN^- and the neutral amide groups. The affinity ratios lead to an interesting scenario: if the measured affinity values of the model compounds are similar to those of functional groups of proteins, the amide groups can bind to the SCN^- anions during protein denaturation with a similar or even larger probability than the positively charged groups if a large number of the amide groups can expose to the water phase during the denaturation. We urge caution here that results from this work are not necessarily immediately transferable to big biomolecules, e.g., proteins, because the formation of a global stable conformation in a protein may impose geometric constraints on some segments. The geometric constraints can block ions from approaching the functional groups of the segments, shifting the chemical equilibrium of ion/segment interactions away from that of the ion/model–molecule interactions free of geometric constraints studied here. For those segments free of geometric constraints, there is no spatial problem for ions to approach the functional groups. We would expect that their interactions with ions should be similar to those studied in this work. Nonetheless, the chemical equilibrium among ion/water/molecule revealed in this work can be potentially helpful for

understanding of molecular structures and dynamics in aqueous solutions.

■ ASSOCIATED CONTENT

Supporting Information

Additional experimental details. This material is available free of charge via the Internet at <http://pubs.acs.org>.

■ AUTHOR INFORMATION

Corresponding Author

*E-mail: junrong@rice.edu.

Notes

The authors declare no competing financial interest.

■ ACKNOWLEDGMENTS

This material is based upon work supported by the Welch foundation under Award No. C-1752 and the Air Force Office of Scientific Research under AFOSR Award No. FA9550-11-1-0070. J. R. Zheng also thanks the David and Lucile Packard Foundation for a Packard fellowship. We also thank Prof. Robert Curl and Philip R. Brooks' for substantial discussions and suggestions and language modifications of the manuscript.

■ ABBREVIATIONS

SCN, thiocyanate; NMA, *N*-methylacetamide; FMA, formamide; DMF, dimethylformamide; DEA, diethylamine

■ REFERENCES

- (1) Vonhippel, P. H.; Wong, K. Y. *Science* **1964**, *145*, 577–580.
- (2) Zhang, Y. J.; Cremer, P. S. *Curr. Opin. Chem. Biol.* **2006**, *10*, 658–663.
- (3) Robinson, D. R.; Jencks, W. P. *J. Am. Chem. Soc.* **1965**, *87*, 2470–2479.
- (4) Scott, J. N.; Nucci, N. V.; Vanderkooi, J. M. *J. Phys. Chem. A* **2008**, *112*, 10939–10948.
- (5) Hippel, P. H. V.; Wong, K. Y. *Biochemistry* **1962**, *1*, 664–674.
- (6) Collins, K. D.; Washabaugh, M. W. *Q. Rev. Biophys.* **1985**, *18*, 323–422.
- (7) Omta, A. W.; Kropman, M. F.; Woutersen, S.; Bakker, H. J. *Science* **2003**, *301*, 347–349.
- (8) Omta, A. W.; Kropman, M. F.; Woutersen, S.; Bakker, H. J. *J. Chem. Phys.* **2003**, *119*, 12457.
- (9) Hamiaux, C.; Prange, T.; Ries-Kautt, M.; Ducruix, A.; Lafont, S.; Astier, J. P.; Veessler, S. *Acta Crystallogr., Sect. D: Biol. Crystallogr.* **1999**, *55*, 103–113.
- (10) Vaney, M. C.; Broutin, I.; Retaillieu, P.; Douangamath, A.; Lafont, S.; Hamiaux, C.; Prange, T.; Ducruix, A.; Ries-Kautt, M. *Acta Crystallogr., Sect. D: Biol. Crystallogr.* **2001**, *57*, 929–940.

- (11) Chakrabarti, P. *J. Mol. Biol.* **1993**, *234*, 463–482.
- (12) Jorgensen, W. L.; Duffy, E. M.; Tiradorives, J. *Philos. Trans. R. Soc. London, A* **1993**, *345*, 87–96.
- (13) Mason, P. E.; Brady, J. W.; Neilson, G. W.; Dempsey, C. E. *Biophys. J.* **2007**, *93*, L4–L6.
- (14) Heyda, J.; Vincent, J. C.; Tobias, D. J.; Dzubiella, J.; Jungwirth, P. *J. Phys. Chem. B* **2010**, *114*, 1213–1220.
- (15) Bian, H. T.; Wen, X. W.; Li, J. B.; Chen, H. L.; Han, S. Z.; Sun, X. Q.; Song, J. A.; Zhuang, W.; Zheng, J. R. *Proc. Natl. Acad. Sci. U.S.A.* **2011**, *108*, 4737–4742.
- (16) Bian, H. T.; Chen, H. L.; Li, J. B.; Wen, X. W.; Zheng, J. R. *J. Phys. Chem. A* **2011**, *115*, 11657–11664.
- (17) Li, J. B.; Bian, H. T.; Chen, H. L.; Zheng, J. R. *J. Phys. Chem. B*, 10.1021/jp3053373.
- (18) Bian, H. T.; Li, J. B.; Zhang, Q.; Chen, H. L.; Zhuang, W.; Gao, Y. Q.; Zheng, J. R., submitted.
- (19) Förster, T. *Ann. Phys.-Berlin* **1948**, *2*, 55–75 (German).
- (20) Bian, H. T.; Li, J. B.; Wen, X. W.; Zheng, J. R. *J. Chem. Phys.* **2010**, *132*, 184505.
- (21) Bian, H. T.; Wen, X. W.; Li, J. B.; Zheng, J. R. *J. Chem. Phys.* **2010**, *133*, 034505.
- (22) Bian, H. T.; Zhao, W.; Zheng, J. R. *J. Chem. Phys.* **2009**, *131*, 124501.
- (23) Sedlak, E.; Stagg, L.; Wittung-Stafshede, P. *Arch. Biochem. Biophys.* **2008**, *479*, 69–73.
- (24) Hess, B.; van der Vegt, N. F. A. *Proc. Natl. Acad. Sci. U.S.A.* **2009**, *106*, 13296–13300.

**Probing Ion/Molecule Interactions in Aqueous Solutions with Vibrational Energy
Transfer**

Jiebo Li, Hongtao Bian, Xiewen Wen, Hailong Chen, Kaijun Yuan, Junrong Zheng*

Department of Chemistry, Rice University, Houston, TX 77005

Supporting materials

This file includes:

Supporting material text

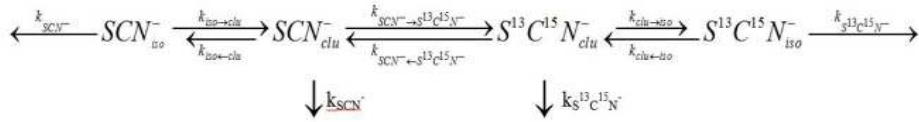
Figure S1 to S17

Table S1 to S5

References

Kinetic model and fitting results

In a KSCN-amino acid -water solution, there are three types of thiocyanate anions: clustered, hydrated (free) and amino acid-complexed. The latter two are considered as the isolated species in the kinetic model, because the vibrational energy transfer among the anions of the isolated species is much slower than that of the clustered under the assumption of dipole-dipole approximation. Based on the physical picture, a kinetic model was constructed to quantitatively analyze the experiments. As shown in Scheme S1, the vibrational excitations of all species decay with their own lifetimes. The clustered anions can exchange their vibrational excitations. At room temperature, the clustered ions and the isolated ions are under dynamic equilibrium¹.



Scheme S1.

From the model, four differential equations are derived as below:

$$\frac{d[SCN_{clu}^-]}{dt} = k_{iso \rightarrow clu} [SCN_{iso}^-] + k_{SCN^- \rightarrow S^{13}C^{15}N^-} [S^{13}C^{15}N_{clu}^-] - (k_{iso \leftarrow clu} + k_{SCN^- \rightarrow S^{13}C^{15}N^-} + k_{SCN^-}) [SCN_{clu}^-] \quad \text{Eq. S1}$$

$$\frac{d[SCN_{iso}^-]}{dt} = k_{iso \leftarrow clu} [SCN_{clu}^-] - (k_{SCN^-} + k_{iso \rightarrow clu}) [SCN_{iso}^-] \quad \text{Eq. S2}$$

$$\frac{d[S^{13}C^{15}N_{clu}^-]}{dt} = k_{iso \rightarrow clu} [S^{13}C^{15}N_{iso}^-] + k_{SCN^- \rightarrow S^{13}C^{15}N^-} [SCN_{clu}^-] - (k_{iso \leftarrow clu} + k_{SCN^- \rightarrow S^{13}C^{15}N^-} + k_{S^{13}C^{15}N^-}) [S^{13}C^{15}N_{clu}^-] \quad \text{Eq. S3}$$

$$\frac{d[S^{13}C^{15}N_{iso}^-]}{dt} = k_{iso \leftarrow clu} [S^{13}C^{15}N_{clu}^-] - (k_{S^{13}C^{15}N^-} + k_{iso \rightarrow clu}) [S^{13}C^{15}N_{iso}^-] \quad \text{Eq. S4}$$

The time dependent populations (isolated SCN^- , clustering SCN , isolated $\text{S}^{13}\text{C}^{15}\text{N}^-$ and clustering $\text{S}^{13}\text{C}^{15}\text{N}^-$) and vibrational lifetimes are experimentally determined. The isolated and clustered species equilibrium constant K ($K = \frac{k_{iso \rightarrow clu}}{k_{iso \leftarrow clu}}$) determine the location exchange rate constant ratio. The energy exchange rate constant ratio D is determined by the energy mismatch of the two vibrations. The normalized initial populations are: $[\text{SCN}_{clu}^-(0)^*] = \frac{K}{K+1}$, $[\text{SCN}_{iso}^-(0)^*] = \frac{1}{K+1}$, $[\text{S}^{13}\text{C}^{15}\text{N}_{clu}^-(0)^*] = [\text{S}^{13}\text{C}^{15}\text{N}_{iso}^-(0)^*] = 0$. Solving equations (Eq. (S1) ~Eq. (S4)) with our experiment results gives the energy transfer rate constants, the isolated-clustered ion equilibrium constant ($k_{iso \rightarrow clu}$ and $k_{iso \leftarrow clu}$) and the isolated/clustered equilibrium constant (K).

For the solutions, the ideal detailed balance of peak 6 and peak 8 is 0.7 due to the energy mismatch 73 cm^{-1} . This can be easily obtained from experiments as the intensity ratio of peak 8 to peak 6 is 0.7. Therefore, D is a constant. Our previous experiments² show that from 4M KSCN aqueous solution to 1.8M solution, the cluster ratio decreases from 67% to 35%. However, the average cluster size remains almost constant (5 to 4). In solutions A~O, most of the cluster ratios are within this range. Therefore, we assume that the cluster size is constant in all solutions so that we can keep the energy transfer rate constants constant for all samples in the calculations to have a fair comparison for the cluster ratios.

Analysis based on experimental results and the kinetic model for solution A gives $k_{\text{SCN}^- \rightarrow \text{S}^{13}\text{C}^{15}\text{N}^-} = 1/140 \text{ (ps}^{-1}\text{)}$. Equilibrium constant K is 2.0, which indicates that the cluster ratio is 67%. The location exchange rate constant is $k_{clu \rightarrow iso} = 1/10 \text{ (ps}^{-1}\text{)}$.

Experimental results and calculations based on the kinetic model with the following parameters are displayed in Figure S1:

$$k_{SCN^-_{fast}} = 1/3.1 (ps^{-1}); k_{SCN^-_{slow}} = 1/30.5 (ps^{-1}); k_{S^{13}C^{15}N^-_{fast}} = 1/2.1 (ps^{-1}); k_{S^{13}C^{15}N^-_{slow}} = 1/25.1 (ps^{-1});$$

$$k_{clu \rightarrow iso} = 1/10 (ps^{-1}); K=2.0; k_{SCN^- \rightarrow S^{13}C^{15}N^-} = 1/140 (ps^{-1}); D=0.7$$

with pre-factors of the subgroups and offset of the bi-exponential

$$A_{SCN^-_{fast}} = 0.05; A_{SCN^-_{slow}} = 0.95; A_{S^{13}C^{15}N^-_{fast}} = 0.07; A_{S^{13}C^{15}N^-_{slow}} = 0.93; offset = 0.$$

For solutions B~O, calculations and experimental results are displayed in Figure S2~S14. Parameters for calculations are listed in the following. Here it is necessary to note that in our experiment, the cross peaks and the diagonal peaks are measured in different laser focusing conditions. For the cross peak measurement, the pump laser beam was focused very tight at the sample because the energy transfer peaks are usually very weak, especially when the amino acids were added to the KSCN/KS¹³C¹⁵N solution. Also we only measured the cross peaks when the pump located at 2060 cm⁻¹ and peak 6 was used to do the energy transfer analysis. While the other cross peaks pair (peak 7 and peak 8) are not measured. Since we already know the detailed balance ratio for the pumping/up and flowing down is 0.7 for the KSCN/KS¹³C¹⁵N solution, we simply scaled the flowing down curves by 0.7 as the pumping up curves in our data analysis. However we cannot use the diagonal peaks to do the vibrational lifetime analysis when the pump laser beam was tightly focused, because high order nonlinear processes may occur for the KSCN solution which may affect the vibrational lifetime analysis. Alternatively, for the vibrational lifetime analysis, we defocused the pump laser beam to eliminate the high order nonlinear processes and the generated pump probe signals are significantly attenuated.

For solution B, the calculation parameters are:

$$k_{SCN^- fast} = 1/1.5 (ps^{-1}); k_{SCN^- slow} = 1/14.5 (ps^{-1}); k_{S^{13}C^{15}N^- fast} = 1/1.1 (ps^{-1}); k_{S^{13}C^{15}N^- slow} = 1/15.0 (ps^{-1});$$
$$k_{clu \rightarrow iso} = 1/10 (ps^{-1}); K=0.92; k_{SCN^- \rightarrow S^{13}C^{15}N^-} = 1/140 (ps^{-1}); D=0.7$$

with pre-factors of the subgroups and offset of the single-exponential

$$A_{SCN^- fast} = 0.15; A_{SCN^- slow} = 0.85; A_{S^{13}C^{15}N^- fast} = 0.10; A_{S^{13}C^{15}N^- slow} = 0.90; offset = 0$$

Solution C:

$$k_{SCN^- fast} = 1/2.5 (ps^{-1}); k_{SCN^- slow} = 1/15.3 (ps^{-1}); k_{S^{13}C^{15}N^- fast} = 1/2.1 (ps^{-1}); k_{S^{13}C^{15}N^- slow} = 1/16.5 (ps^{-1});$$
$$k_{clu \rightarrow iso} = 1/6 (ps^{-1}); K=0.51; k_{SCN^- \rightarrow S^{13}C^{15}N^-} = 1/140 (ps^{-1}); D=0.7$$

with pre-factors of the subgroups and offset of the bi-exponential

$$A_{SCN^- fast} = 0.08; A_{SCN^- slow} = 0.92; A_{S^{13}C^{15}N^- fast} = 0.15; A_{S^{13}C^{15}N^- slow} = 0.85; offset = 0$$

Solution D:

$$k_{SCN^- fast} = 1/1.26 (ps^{-1}); k_{SCN^- slow} = 1/14.2 (ps^{-1}); k_{S^{13}C^{15}N^- fast} = 1/1.3 (ps^{-1}); k_{S^{13}C^{15}N^- slow} = 1/18.0 (ps^{-1});$$
$$k_{clu \rightarrow iso} = 1/10 (ps^{-1}); K=0.82; k_{SCN^- \rightarrow S^{13}C^{15}N^-} = 1/140 (ps^{-1}); D=0.7$$

with pre-factors of the subgroups and offset of the bi-exponential

$$A_{SCN^- fast} = 0.085; A_{SCN^- slow} = 0.915; A_{S^{13}C^{15}N^- fast} = 0.116; A_{S^{13}C^{15}N^- slow} = 0.884; offset = 0$$

Solution E:

$$k_{SCN^- fast} = 1/1.7 (ps^{-1}); k_{SCN^- slow} = 1/16.5 (ps^{-1}); k_{S^{13}C^{15}N^- fast} = 1/2.6 (ps^{-1}); k_{S^{13}C^{15}N^- slow} = 1/17.8 (ps^{-1});$$
$$k_{clu \rightarrow iso} = 1/10 (ps^{-1}); K=0.60; k_{SCN^- \rightarrow S^{13}C^{15}N^-} = 1/145 (ps^{-1}); D=0.7$$

with pre-factors of the subgroups and offset of the bi-exponential

$$A_{SCN^- fast} = 0.04; A_{SCN^- slow} = 0.96; A_{S^{13}C^{15}N^- fast} = 0.17; A_{S^{13}C^{15}N^- slow} = 0.83; offset = 0$$

Solution F

$$k_{SCN^- fast} = 1/1.26 (ps^{-1}); k_{SCN^- slow} = 1/13.0 (ps^{-1}); k_{S^{13}C^{15}N^- fast} = 1/1.30 (ps^{-1}); k_{S^{13}C^{15}N^- slow} = 1/13.1 (ps^{-1});$$
$$k_{clu \rightarrow iso} = 1/10 (ps^{-1}); K=0.42; k_{SCN^- \rightarrow S^{13}C^{15}N^-} = 1/140 (ps^{-1}); D=0.7$$

with pre-factors of the subgroups and offset of the bi-exponential

$$A_{SCN^- fast} = 0.085; A_{SCN^- slow} = 0.915; A_{S^{13}C^{15}N^- fast} = 0.116; A_{S^{13}C^{15}N^- slow} = 0.884; offset = 0$$

Solution G:

$$k_{SCN^- fast} = 1/1.75(ps^{-1}); k_{SCN^- slow} = 1/31.56(ps^{-1}); k_{S^{13}C^{15}N^- fast} = 1/2.11(ps^{-1}); k_{S^{13}C^{15}N^- slow} = 1/34.45(ps^{-1});$$

$$k_{clu \rightarrow iso} = 1/10(ps^{-1}); K=1.85; k_{SCN^- \rightarrow S^{13}C^{15}N^-} = 1/140(ps^{-1}); D=0.7$$

with pre-factors of the subgroups and offset of the bi-exponential

$$A_{SCN^- fast} = 0.085; A_{SCN^- slow} = 0.915; A_{S^{13}C^{15}N^- fast} = 0.116; A_{S^{13}C^{15}N^- slow} = 0.884; offset = 0$$

Solution H:

$$k_{SCN^- fast} = 0(ps^{-1}); k_{SCN^- slow} = 1/17.2(ps^{-1}); k_{S^{13}C^{15}N^- fast} = 0(ps^{-1}); k_{S^{13}C^{15}N^- slow} = 1/16.2(ps^{-1});$$

$$k_{clu \rightarrow iso} = 1/10(ps^{-1}); K=0.85; k_{SCN^- \rightarrow S^{13}C^{15}N^-} = 1/140(ps^{-1}); D=0.7$$

with pre-factors of the subgroups and offset of the bi-exponential

$$A_{SCN^- fast} = 0.0; A_{SCN^- slow} = 1; A_{S^{13}C^{15}N^- fast} = 0; A_{S^{13}C^{15}N^- slow} = 1; offset = 0$$

Solution J:

$$k_{SCN^- fast} = 1/4.5(ps^{-1}); k_{SCN^- slow} = 1/26.0(ps^{-1}); k_{S^{13}C^{15}N^- fast} = 1/4.0(ps^{-1}); k_{S^{13}C^{15}N^- slow} = 1/27.5(ps^{-1});$$

$$k_{clu \rightarrow iso} = 1/10(ps^{-1}); K=1.28; k_{SCN^- \rightarrow S^{13}C^{15}N^-} = 1/140(ps^{-1}); D=0.7$$

with pre-factors of the subgroups and offset of the bi-exponential

$$A_{SCN^- fast} = 0.12; A_{SCN^- slow} = 0.88; A_{S^{13}C^{15}N^- fast} = 0.08; A_{S^{13}C^{15}N^- slow} = 0.92; offset = 0$$

Solution K:

$$k_{SCN^- fast} = 1/1.26(ps^{-1}); k_{SCN^- slow} = 1/22.90(ps^{-1}); k_{S^{13}C^{15}N^- fast} = 1/1.3(ps^{-1}); k_{S^{13}C^{15}N^- slow} = 1/23.25(ps^{-1});$$

$$k_{clu \rightarrow iso} = 1/10(ps^{-1}); K=1.0; k_{SCN^- \rightarrow S^{13}C^{15}N^-} = 1/140(ps^{-1}); D=0.7$$

with pre-factors of the subgroups and offset of the bi-exponential

$$A_{SCN^- fast} = 0.085; A_{SCN^- slow} = 0.915; A_{S^{13}C^{15}N^- fast} = 0.126; A_{S^{13}C^{15}N^- slow} = 0.874; offset = 0$$

Solution L:

$$k_{SCN^- fast} = 1/1.26(ps^{-1}); k_{SCN^- slow} = 1/21.90(ps^{-1}); k_{S^{13}C^{15}N^- fast} = 1/1.3(ps^{-1}); k_{S^{13}C^{15}N^- slow} = 1/29.0(ps^{-1});$$

$$k_{clu \rightarrow iso} = 1/10(ps^{-1}); K=1.74; k_{SCN^- \rightarrow S^{13}C^{15}N^-} = 1/140(ps^{-1}); D=0.7$$

with pre-factors of the subgroups and offset of the bi-exponential

$$A_{SCN^- fast} = 0.085; A_{SCN^- slow} = 0.915; A_{S^{13}C^{15}N^- fast} = 0.116; A_{S^{13}C^{15}N^- slow} = 0.884; offset = 0$$

Solution M:

$$k_{SCN^- fast} = 1/1.26(ps^{-1}); k_{SCN^- slow} = 1/28.00(ps^{-1}); k_{S^{13}C^{15}N^- fast} = 1/1.3(ps^{-1}); k_{S^{13}C^{15}N^- slow} = 1/33.0(ps^{-1});$$

$$k_{clu \rightarrow iso} = 1/10(ps^{-1}); K=1.52; k_{SCN^- \rightarrow S^{13}C^{15}N^-} = 1/140(ps^{-1}); D=0.7$$

with pre-factors of the subgroups and offset of the bi-exponential

$$A_{SCN^- fast} = 0.085; A_{SCN^- slow} = 0.915; A_{S^{13}C^{15}N^- fast} = 0.116; A_{S^{13}C^{15}N^- slow} = 0.884; offset = 0$$

Solution N:

$$k_{SCN^- slow} = 1 / 20 (ps^{-1}); k_{S^{13}C^{15}N^- slow} = 1 / 24.8 (ps^{-1});$$
$$k_{clu \rightarrow iso} = 1 / 10 (ps^{-1}); K = 1.05; k_{SCN^- \rightarrow S^{13}C^{15}N^-} = 1 / 140.0 (ps^{-1});$$

with pre-factors of the subgroups and offset of the bi-exponential

$$A_{SCN^- fast} = 0.0; A_{SCN^- slow} = 1; A_{S^{13}C^{15}N^- fast} = 0.0; A_{S^{13}C^{15}N^- slow} = 1.0; offset = 0$$

Solution O:

$$k_{SCN^- fast} = 1 / 2.9 (ps^{-1}); k_{SCN^- slow} = 1 / 19.70 (ps^{-1}); k_{S^{13}C^{15}N^- fast} = 1 / 1.80 (ps^{-1}); k_{S^{13}C^{15}N^- slow} = 1 / 21.98 (ps^{-1});$$
$$k_{clu \rightarrow iso} = 1 / 10 (ps^{-1}); K = 1.10; k_{SCN^- \rightarrow S^{13}C^{15}N^-} = 1 / 140 (ps^{-1}); D = 0.7$$

with pre-factors of the subgroups and offset of the bi-exponential

$$A_{SCN^- fast} = 0.10; A_{SCN^- slow} = 0.90; A_{S^{13}C^{15}N^- fast} = 0.14; A_{S^{13}C^{15}N^- slow} = 0.86; offset = 0$$

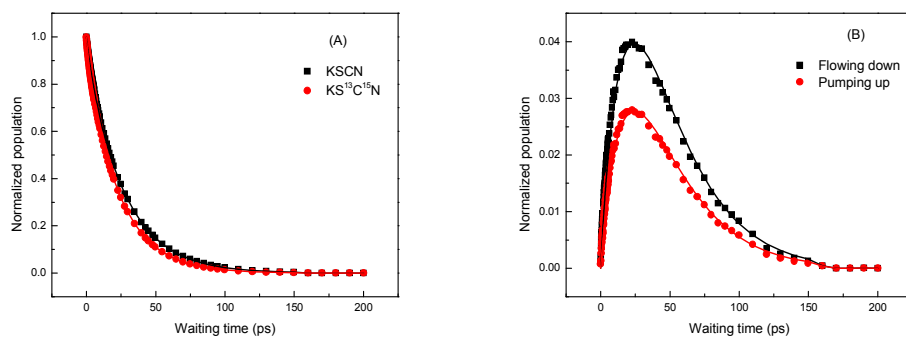


Figure S1. Data and calculations of **Solution A** (4.0M KSCN/ $\text{KS}^{13}\text{C}^{15}\text{N}$ D_2O solution); Dots are data, and lines are calculations.

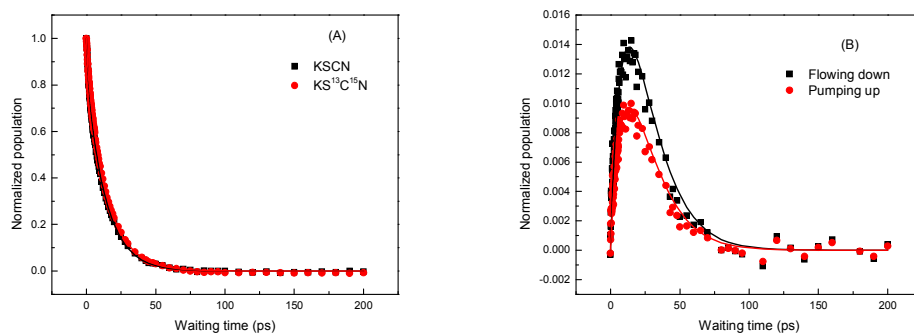


Figure S2. Data and calculations of **Solution B** (Pro:KSCN: $\text{KS}^{13}\text{C}^{15}\text{N}$: D_2O = 1:1:1:20). Dots are data, and lines are calculations

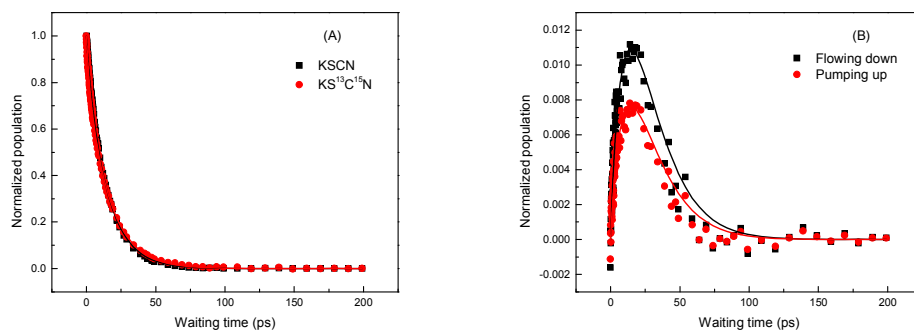


Figure S3. Data and calculations of **Solution C** (Pro:KSCN: $\text{KS}^{13}\text{C}^{15}\text{N}$: D_2O = 2:1:1:20). Dots are data, and lines are calculations

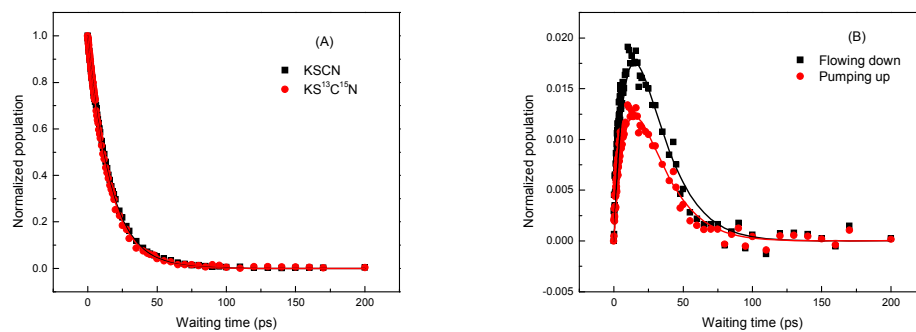


Figure S4. Data and calculations of **Solution D** (Gly:KSCN:KS¹³C¹⁵N:D₂O=1:1:1:20). Dots are data, and lines are calculations.

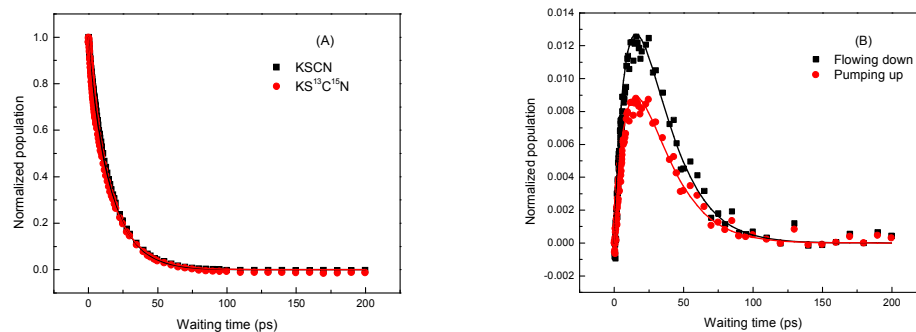


Figure S5. Data and calculations of **Solution E** (Cys:KSCN:KS¹³C¹⁵N:D₂O =1:1:1:20). Dots are data, and lines are calculations.

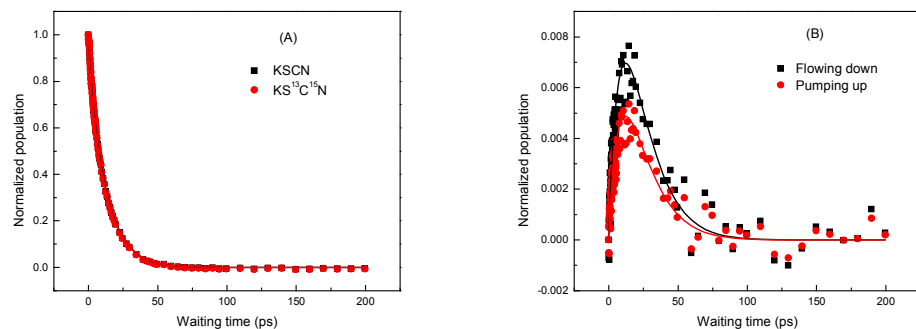


Figure S6. Data and calculations of **Solution F** (Lys:KSCN:KS¹³C¹⁵N:D₂O =1:1:1:20). Dots are data, and lines are calculations.

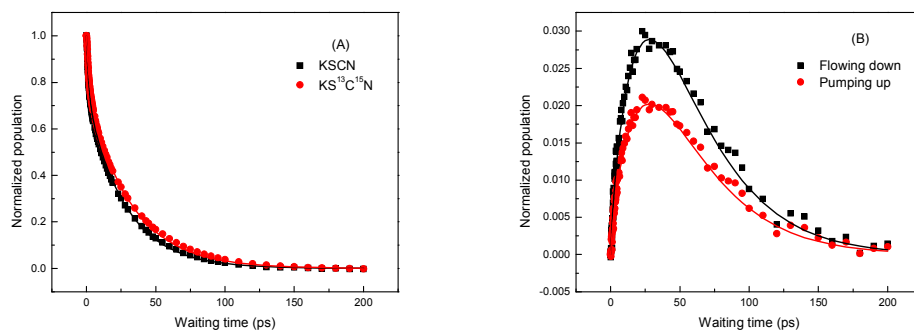


Figure S7. Data and calculations of **Solution G** ($\text{CH}_3\text{COOK}:\text{KSCN}:\text{KS}^{13}\text{C}^{15}\text{N}:\text{D}_2\text{O}$ =2:1:1:20). Dots are data, and lines are calculations.

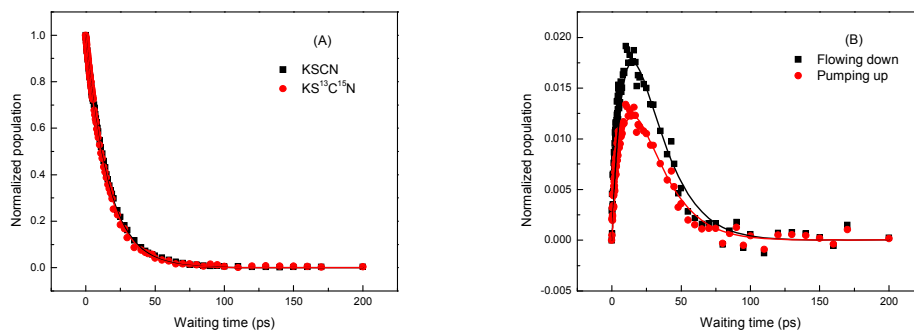


Figure S8. Data and calculations of **Solution H** ($\text{CH}_3\text{NH}_3\text{Cl}:\text{KSCN}:\text{KS}^{13}\text{C}^{15}\text{N}:\text{D}_2\text{O}$ =1:1:1:20). Dots are data, and lines are calculations.

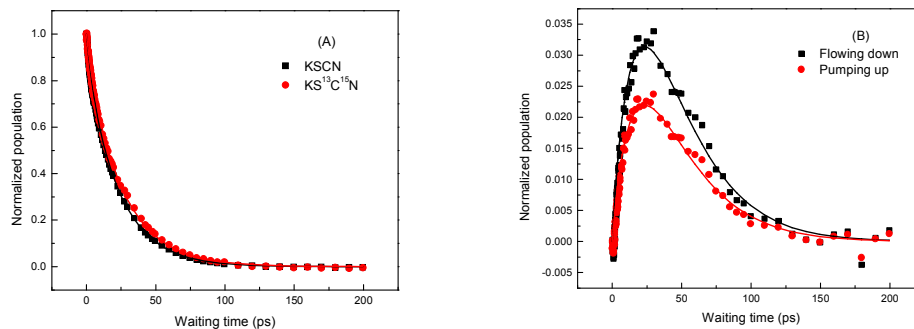


Figure S9. Data and calculations of **Solution J** ($\text{NMA}:\text{KSCN}:\text{KS}^{13}\text{C}^{15}\text{N}:\text{D}_2\text{O}$ =2:1:1:20). Dots are data, and lines are calculations.

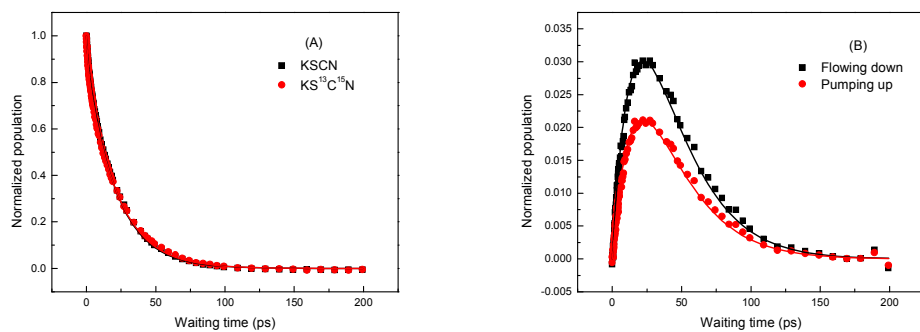


Figure S10. Data and calculations of **Solution K** (NMA:KSCN:KS¹³C¹⁵N:D₂O =4:1:1:20). Dots are data, and lines are calculations.

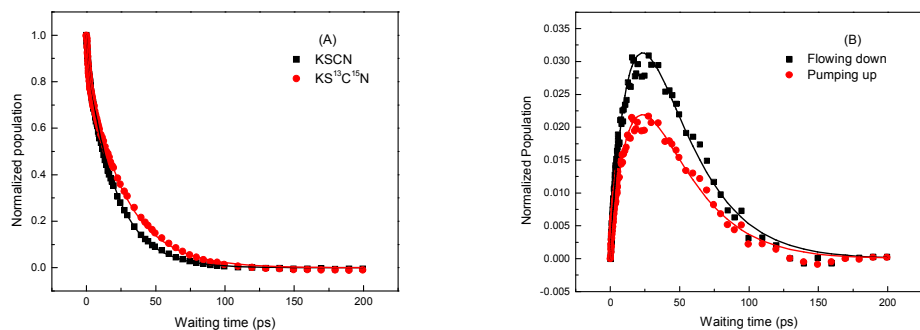


Figure S11. Data and calculations of **Solution L** (Acetone:KSCN:KS¹³C¹⁵N:D₂O =2:1:1:20). Dots are data, and lines are calculations.

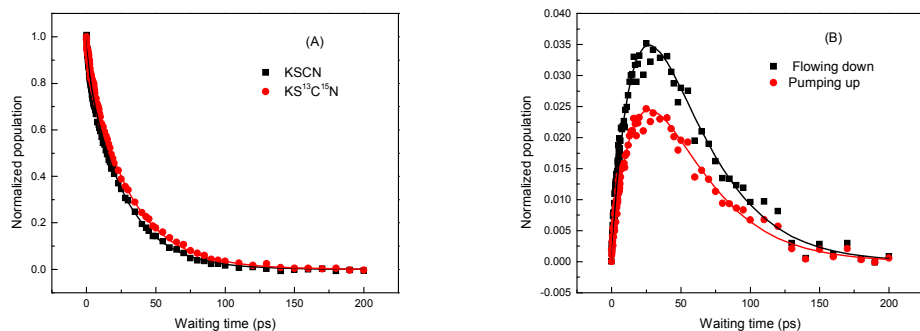


Figure S12. Data and calculations of **Solution M** (DMF:KSCN:KS¹³C¹⁵N:D₂O =2:1:1:20). Dots are data, and lines are calculations.

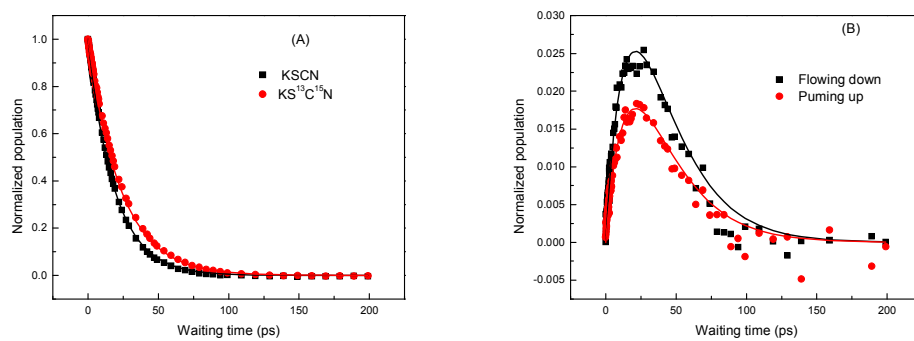


Figure S13. Data and calculations of **Solution N** ($\text{HCONH}_2:\text{KSCN}:\text{KS}^{13}\text{C}^{15}\text{N}:\text{D}_2\text{O}$ =2:1:1:20). Dots are data, and lines are calculations.

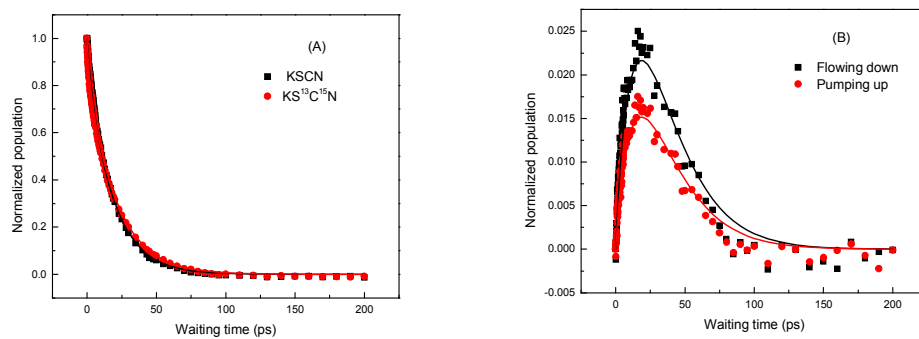


Figure S14. Data and calculations of **Solution O** ($(\text{C}_2\text{H}_5)_2\text{NH}:\text{KSCN}:\text{KS}^{13}\text{C}^{15}\text{N}:\text{D}_2\text{O}$ =2:1:1:20). Dots are data, and lines are calculations.

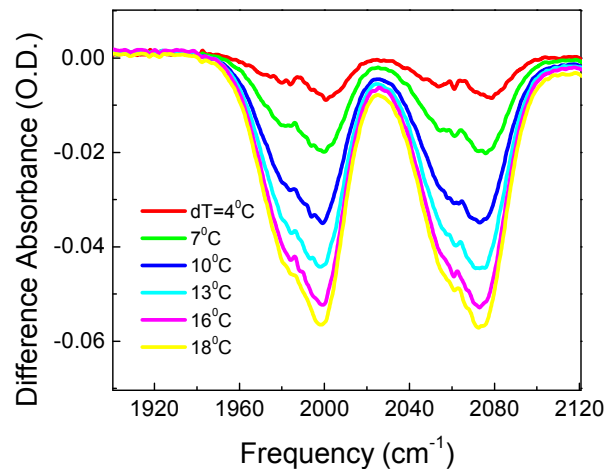


Figure S15. The temperature difference FTIR spectra of the 4M KSCN/KS¹³C¹⁵N=1/1 D₂O solution. Each colored line represents the absorbance difference (high temperature - low temperature) between a measurement at a higher temperature and the measurement at room temperature. Negative value represents bleaching. Heating induces obvious bleachings near the 0-1 transition frequencies (~2066 and 1993 cm⁻¹) of the nitrile stretches. The effect near the 1-2 transition frequencies (~2040 and 1965 cm⁻¹) is much smaller. In 2D IR measurements, the heat from vibrational relaxations increases the temperature of the sample. Because the 2D IR spectra are the difference intensity between experiments with excitation on and off, the heat effect is similar to the temperature difference FTIR spectra shown here. In our setup, the temperature increase from vibrational relaxations is only a few degrees.

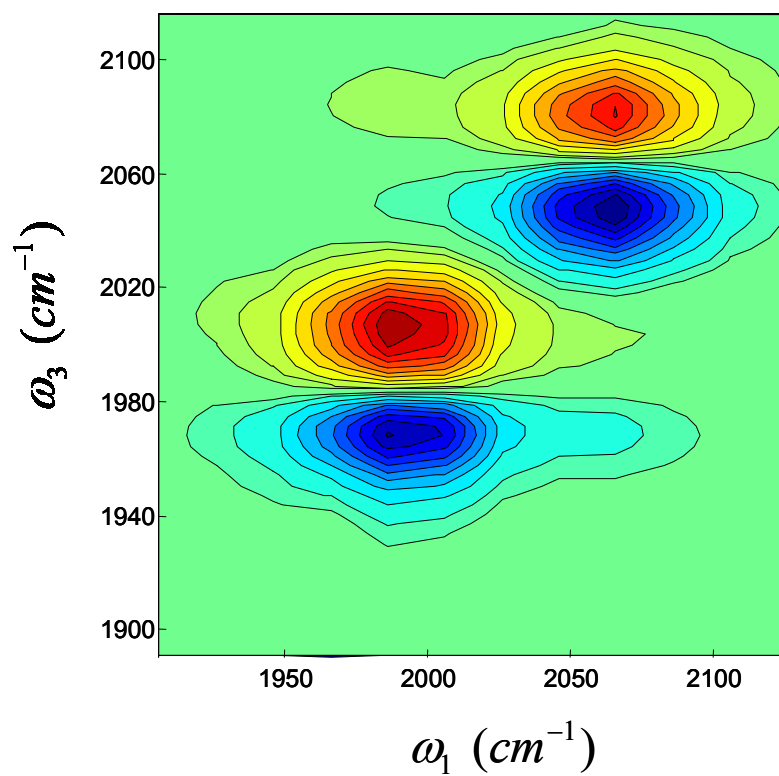


Figure S16. 2D IR spectrum at 30 ps of potassium-H₂O-D₂O (1:1:10) solution. No OH induced heat effect is observed in peaks 5 and 7.

Equilibrium constant calculation

To quantitatively describe the relative binding affinity of the model compounds to the thiocyanate anions, we constructed an equilibrium model to analyze the vibrational energy exchange results. Using **Solution C** as an example, three types of thiocyanate anions coexist under chemical equilibrium: clustered ($SCN_{clustered}^-$), hydrated ($SCN_{hydrated}^-$) and proline-complexed (SCN_{pro}^-). Two types of proline molecules coexist: hydrated ($pro_{hydrated}$) and thiocyanate-complexed (pro_{SCN^-}). We defined these three species based on the experimental observable – vibrational energy transfer: (1) those anions that can transfer energy to other anions are defined as clustered; (2) those anions that can't transfer energy to other anions, which is caused by binding to water, are defined by hydrated; (3) those anions that can't transfer energy, which is caused by binding to model compounds, are defined by compound-complexed. They are not directly related to the physical contact. For example, some water molecules can directly contact S of SCN^- , but these molecules can't block the CN energy transfer. Therefore, these molecules are not considered as those water molecules “hydrate” the SCN^- in the model.

The binding affinity between thiocyanate and proline is defined as

$$K_{affinity} = \frac{[SCN_{pro}^-][D_2O]^n}{[SCN_{hydrated}^-][pro_{hydrated}]}, \quad \text{Eq.S5}$$

from the following equilibrium,



In the model, we considered the self-associated proline molecules as the hydrated species. The total concentration of water was taken as constant since the amount of

additive is relatively small, leading to a constant concentration of hydrated thiocyanate anions. In this approximation, proline/thiocyanate complexes in both water and ion clusters are mathematically combined into one parameter: SCN_{pro}^- . The concentration sum of proline-complexed and hydrated thiocyanate anions was obtained from the vibrational energy exchange experiments, and the concentration of proline was known beforehand. Eq.S6 is readily solvable with all these parameters known. The number of water molecules in Eq.S6 was set to be 1 for comparison of the one-to-one binding affinity.

Using refractive index (table S2) and transition dipole moment correction (table S3), all available $K_{affinity}$ values are listed in Table 1 in the main text and table S4. Two calculations are showed in the following:

Solution B: potassium thiocyanate-proline-D₂O=1-0.5-10. The concentration of potassium is 4M. Cluster ratio is 48%.

$$\begin{aligned}
 [SCN^-]_{total} &= 4.00M; [Pro]_{total} = 2.00M; \\
 \Delta [SCN^-]_{Cluster} &= [SCN^-]_{Pro} = 4.00 - 1.92 - 1.32 = 0.76M; [D_2O]_{total} = 40.00M; \\
 [D_2O]_{Pro} &= [Pro]_{D_2O} = [Pro]_{total} - [Pro]_{SCN^-} = 2.00 - 0.76 = 1.24M; [D_2O]_{Bulk} = 38.76M; \\
 K_{affinity} &= \frac{[SCN^-]_{Pro} [D_2O]_{Bulk}}{[Pro]_{D_2O} [SCN^-]_{hydrated}} = \frac{0.76 \times 38.76}{1.24 \times 1.32} = 18.00
 \end{aligned}$$

Solution O: potassium thiocyanate-(C₂H₅)₂NH-D₂O=1-1-10. The concentration of KSCN is 4M. Cluster ratio is 52%.

$$\begin{aligned}
 [SCN^-]_{total} &= 4.00M; [(C_2H_5)_2NH]_{total} = 4.00M; \\
 \Delta [SCN^-]_{Cluster} &= [SCN^-]_{(C_2H_5)_2NH} = 4.00 - 2.08 - 1.32 = 0.60M; [D_2O]_{total} = 40.00M; \\
 [D_2O]_{(C_2H_5)_2NH} &= [(C_2H_5)_2NH]_{D_2O} = [(C_2H_5)_2NH]_{total} - [(C_2H_5)_2NH]_{SCN^-} = 4.00 - 0.60 = 3.40M; [D_2O]_{Bulk} = 36.60M; \\
 K_{affinity} &= \frac{[SCN^-]_{(C_2H_5)_2NH} [D_2O]_{Bulk}}{[(C_2H_5)_2NH]_{D_2O} [SCN^-]_{hydrated}} = \frac{0.60 \times 36.60}{3.40 \times 1.32} = 4.89
 \end{aligned}$$

Table S1. Cluster ratios of different samples before IR cross section and refractive index corrections

Samples	Cluster ratio
Solution A	67%±2%
Solution B	48%±4%
Solution C	34%±5%
Solution D	45%±4%
Solution E	38%±5%
Solution F	30%±7%
Solution G	65%±4%
Solution H	46%±4%
Solution J	56%±4%
Solution K	50%±4%
Solution L	64%±4%
Solution M	61%±4%
Solution N	51%±4%
Solution O	52%±4%

Solution A (Pro:KSCN:KS¹³C¹⁵N:D₂O =0:1:1:20);

Solution B (Pro:KSCN:KS¹³C¹⁵N:D₂O =1:1:1:20);

Solution C (Pro:KSCN:KS¹³C¹⁵N:D₂O =2:1:1:20);

Solution D (Gly:KSCN:KS¹³C¹⁵N:D₂O=1:1:1:20);

Solution E (Cys:KSCN:KS¹³C¹⁵N:D₂O =1:1:1:20);

Solution F (Lys:KSCN:KS¹³C¹⁵N:D₂O =1:1:1:20);

Solution G (CH₃COOK:KSCN:KS¹³C¹⁵N:D₂O =2:1:1:20);

Solution H (CH₃NH₃Cl:KSCN:KS¹³C¹⁵N:D₂O =1:1:1:20);

Solution J (NMA:KSCN:KS¹³C¹⁵N:D₂O =2:1:1:20);

Solution K (NMA:KSCN:KS¹³C¹⁵N:D₂O =4:1:1:20);

Solution L (Acetone:KSCN:KS¹³C¹⁵N:D₂O =2:1:1:20);

Solution M (DMF:KSCN:KS¹³C¹⁵N:D₂O =2:1:1:20);

Solution N (HCONH₂:KSCN:KS¹³C¹⁵N:D₂O =2:1:1:20);

Solution O ((C₂H₅)₂NH:KSCN:KS¹³C¹⁵N:D₂O =2:1:1:20);

Local refractive index corrections

As mentioned in the main text, adding another species into the potassium thiocyanate aqueous solutions will inevitably change the refractive indexes of the solutions and the transition dipole moments of the nitrile stretches if the additives can interact with the thiocyanate anions. According to the vibrational energy transfer equation and the dipole/dipole approximation, shown in Eq.S7&S8, these two factors can also affect the vibrational energy transfer rates, in addition to the ion cluster concentration:

$$k_{DA} = \frac{1}{1 + e^{-\frac{\Delta\omega_{DA}}{RT}}} \langle \beta \rangle^2 \frac{\frac{1}{\tau_c}}{\left(\frac{1}{\tau_c}\right)^2 + (\Delta\omega_{DA})^2}, \quad \text{Eq.S7}$$

where k_{DA} is the energy transfer rate constant from the donor (D) to the acceptor (A). $\Delta\omega_{DA} = \omega_D - \omega_A$ is the frequency difference between the donor and the acceptor. R is the gas constant. T is the temperature. $\langle \beta \rangle$ is the average coupling constant between D and A. τ_c is the coupling fluctuation time. For all the room temperature liquids we studied so far, τ_c was found to be $2.0 \pm 0.1 ps$. This is at the same time scale as that of solvent molecules reorganizing their configurations, corresponding to the molecular binding enthalpy ~ 0.6 kcal/mol which is the same as the thermal energy at room temperature. $\left(\frac{1}{\tau_c}\right)^2$ is in the energy or frequency unit corresponding to each τ_c .

The coupling between two dipoles is given by

$$\begin{aligned} \langle \beta \rangle &= \frac{1}{4\pi\epsilon_0 n^2} \left[\frac{\boldsymbol{\mu}_D \cdot \boldsymbol{\mu}_A}{r_{DA}^3} - 3 \frac{(\boldsymbol{\mu}_D \cdot \mathbf{r}_{DA})(\boldsymbol{\mu}_A \cdot \mathbf{r}_{DA})}{r_{DA}^5} \right] \\ &= \frac{1}{4\pi\epsilon_0 n^2} \frac{\mu_D \mu_A \kappa}{r_{DA}^3}, \end{aligned} \quad \text{Eq.S8}$$

where ϵ_0 is vacuum permittivity, n is the local refractive index of the media, $\kappa = \cos\theta_{DA} - 3\cos\theta_D \cos\theta_A$, θ_{AD} is the angle between the two transition dipole moments and θ_A and θ_D are the angles between each transition moment and the vector connecting them. $\boldsymbol{\mu}_D$ and $\boldsymbol{\mu}_A$ are the transition dipole moments of donor and acceptor, respectively. r_{DA} is the distance between the donor and acceptor.

Therefore, the variations of transition dipole moments and local refractive indexes induced by the additions of molecules need to be corrected before the concentration of clustered ions can be finally obtained from the energy transfer measurements.

The refractive indexes of KSCN/D₂O (1/10, 4M), (1/7.5, ~5M) and (1/5, 6.5M) solutions were calculated to be 1.41, 1.43, and 1.46 respectively, according to literature.³ We used Eq. S9&S10 to estimate the refractive indexes of solutions with different model compounds with a molecule/salt/water molar ratio 1/1/10:

$$n_{sol} = 1.41 + 0.05 \times \frac{n_{compound} - 1.41}{n_{KSCN} - 1.41}, \quad \text{Eq.S9}$$

and another equation for solutions with compounds with molecule/salt/water molar ratio 0.5/1/10:

$$n_{sol} = 1.41 + 0.02 \times \frac{n_{compound} - 1.41}{n_{KSCN} - 1.41}. \quad \text{Eq.S10}$$

The refractive index of KSCN at 5 microns is 1.53. For most of the compounds, the refractive indexes at 5 microns are not available from literature. Instead, we use the values at ~600nm reported in references⁴⁻¹⁰. In these compounds, refractive index of

the $\text{NH}_3\text{CH}_3\text{Cl}$ is not available. We took the value 1.44 that comes from the compound $\text{NH}_2(\text{CH}_3)_2\text{Cl}$ instead. This can cause about 0.5% - 1% uncertainty (estimated from the frequency dependent of refractive indexes of KI, KF, NaCl) in the final results. Corrected results are displayed in table S2. The refractive index changes are smaller than 1.5%, within this range: 1.41 ± 0.2 , except for the KSCN:Pro:D₂O= 1:1:10 of which $n = 1.44$.

Table S2. Refractive indexes of solutions

	Refractive index (pure compound)	Sample	Refractive index (solution)
Glycine	1.500	KSCN:Gly:D ₂ O= 0.5:1:10	1.42
Proline	1.487	KSCN:Pro:D ₂ O =0.5:1:10 KSCN:Pro:D ₂ O= 1:1:10	1.42 1.44
Lysine	1.503	KSCN:Lys:D ₂ O =0.5:1:10	1.43
NMA	1.428	KSCN:NMA:D ₂ O= 1:1:10 KSCN:NMA:D ₂ O= 2:1:10	1.41 1.42
Formamide	1.447	KSCN:FMA:D ₂ O =0.5:1:10	1.42
CH ₃ COOK	1.370	KSCN:Ack:D ₂ O =1:1:10	1.39
Acetone	1.360	KSCN:Acetone:D ₂ O= 1:1:10	1.39
Diethylamide	1.385	KSCN:DAM:D ₂ O =1:1:10	1.40
DMF	1.431	KSCN:DMF:D ₂ O =1:1:10	1.42
Diethylamine	1.385	KSCN: DEA :D ₂ O= 1:1:10 KSCN: DEA :D ₂ O= 1:1:10	1.41 1.40
NH ₃ CH ₃ Cl	1.44	KSCN:NH ₃ CH ₃ Cl:D ₂ O=1:0.5:10	1.42

Transition dipole moment correction

The nitrile stretch 0-1 transition dipole moment changes induced by the addition of model compounds were determined in the following procedure. A model compound and water were mixed with a certain molar ratio to match that of the sample in 2D IR measurements. FTIR spectrum was taken from this mixture as the background. KSCN was then added into the mixture with a molar ratio 1/200 (KSCN/water). FTIR spectra of this sample and a solution KSCN/water (=1/200) were then measured. The density of each sample was measured to normalize the number of KSCN in the optical path. The change of the CN transition dipole moment square is then proportional to the intensity change of CN stretch peak 2065 cm^{-1} between with and without the model compound. The uncertainty of the measurements was estimated to be ~5%. The change given by this method is the maximum change the nitrile stretch can have. In the 2D IR samples, because the KSCN concentration is much higher, the change is expected to be smaller. At the concentrations of 2D IR samples, the FTIR measurements could not be reliably repeated because of the very small optical path, 1~2 microns. The measured values of $\left(\frac{\mu_{\text{mixture}}}{\mu_{\text{KSCN}}}\right)^2$ are listed in table S3. The transition dipole moments in most mixtures are smaller than that of the KSCN solution for less than 10%.

Table S3. Transition dipole changes

Samples	$\left(\frac{\mu_{mixture}}{\mu_{KSCN}}\right)^2$
KSCN:Proline:H ₂ O=0.5:1:10	0.98
KSCN:Proline: H ₂ O =1.0:1:10	0.91
KSCN:Cysteine: H ₂ O =0.5:1:10	0.92
KSCN:Glycine: H ₂ O =0.5:1:10	0.92
KSCN:Lysine: H ₂ O =0.5:1:10	0.85
KSCN:NMA: H ₂ O =1:1:10	0.92
KSCN:NMA: H ₂ O =2:1:10	0.90
KSCN:Acetone: H ₂ O =1:1:10	1.05
KSCN:Formamide: H ₂ O =0.5:1:10	0.98
KSCN:diethylamide: H ₂ O =1:1:H ₂ O	1.02
KSCN:DMF: H ₂ O =1:1:10	0.97
KSCN:AcK: H ₂ O =1:1:10	0.93
KSCN:NH ₃ CH ₃ Cl: H ₂ O =1:1:10	0.91

Corrections for transition dipole moment and local refractive index

Eq.S7&S8 can be simplified as

$$k_{DA} \propto \frac{\mu_D^2 \mu_A^2}{n^4} = \frac{\mu_{CN}^4}{n^4}. \quad \text{Eq.S11}$$

The change of refractive index is small (<2%). It does not induce a big uncertainty to use the estimated average refractive indexes in table S2 to calculate k_{DA} . However, it can be problematic if the average transition moment changes in table S3 are used because the transition dipole moment changes can be big, up to 10%. Assuming that the transition dipole moment change induced by the addition of a compound is due to the dipole/dipole interaction, this effect is a very short range interaction. According to the dipole/dipole interaction equation Eq.S8, the compound will have very little effect on SCN^- anions which are separated away from this model compound by one other molecule or anion. This situation means that for those SCN^- anions of which the energy exchange can produce visible cross peaks in 2D IR measurements are hardly affected by the addition of the model compound, because they don't directly contact the model compound. Now this will create an interesting situation in the 2D IR spectra. The diagonal peaks are from all SCN^- anions, so that their signals are proportional to the fourth power of the measured average transition dipole moment. However, the cross peaks will be proportional to the fourth power of the transition dipole moment of the clustered anions of which the transition dipole moment is hardly affected by the model compound. The proper kinetic analysis requires the normalization for the difference of transition dipole moments. In reality, it is quite possible that the clustered anions can also be affected by the model compound with a smaller effect. We tested two models to

do the correction: 1. the transition dipole moment of clustered anions is not affected by the addition of a model compound. The peak intensities were renormalized and the calculated cluster concentration and affinity values are listed in table S4. 2. The transition dipole moment of the clustered anions is affected by the addition of a model compound, and the effect is 50% of the measured average effect. The peak intensities were then renormalized accordingly and the energy transfer rate was also normalized with this transition dipole moment change. The calculated cluster concentration and affinity values are listed in table S4. We believe that the 2nd treatment is closer to the real situation and the results are reported, but both treatments give essentially the same conclusion.

Table S4. Corrected affinities with method 1&2 and refractive index

	Original concentration	Original affinity	concentration Corrected	Affinity corrected
Pro:KSCN:D ₂ O 0.5:1:10	48%	18	Method 1: 44% Method 2: 44%	25.1 25.1
Pro:KSCN: D ₂ O 1:1:10	34%	14	Method 1: 29% Method 2: 35%	17.4 13.3
Gly:KSCN: D ₂ O 0.5:1:10	45%	23	Method 1: 38% Method 2: 44%	41.0 25.1
Cys:KSCN: D ₂ O 0.5:1:10	38%	41	Method 1: 31% Method 2: 35%	76.8 52.9
Lys:KCN: D ₂ O 0.5:1:10	30%	85	Method 1: 24% Method 2: 32%	185 69.6
AcK:KSCN: D ₂ O 1:1:10	65%	1	Method 1: 55% Method 2: 62%	3.8 1.4
CH ₃ NH ₃ Cl:KSCN: D ₂ O 0.5:1:1	46%	21	Method 1: 38% Method 2: 44%	40.9 25.1
NMA:KSCN: D ₂ O 1:1:10	56%	3.5	Method 1: 50% Method 2: 58%	5.7 2.7
Acetone:KSCN: D ₂ O 1:1:10	64%	1	Method 1: 66% Method 2: 62%	0.3 1.4
DMF:KSCN: D ₂ O 1:1:10	61%	2	Method 1: 56% Method 2: 58%	3.4 2.7
DEA:KSCN: D ₂ O 1:1:10	52%	5	Method 1: 55% Method 2: 52%	3.8 4.9
FMA:KSCN: D ₂ O 1:1:10	51%	5	Method 1: 49% Method 2: 52%	6.1 4.9

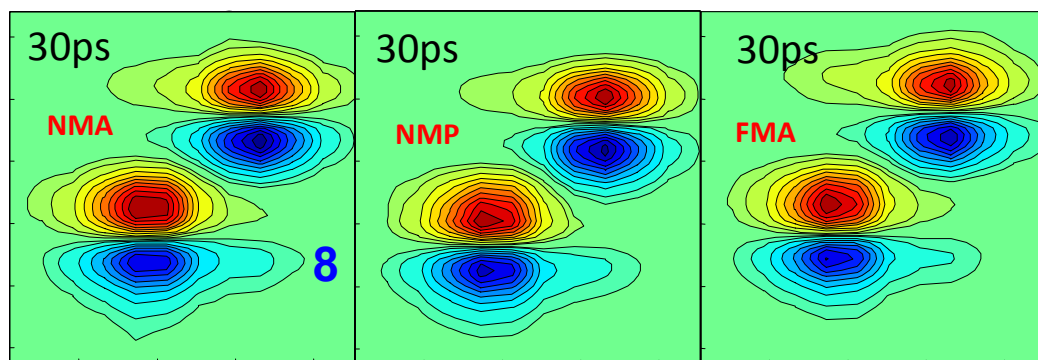


Figure S17. 2D IR spectra at 30 ps of potassium aqueous solutions with the same amount of model compounds: NMA ($\text{CH}_3\text{CONHCH}_3$), NMP (HCONHCH_3), and FMA (HCONH_2). With the number of CH_3 group decreasing, the intensity of peak 8 also decreases, indicating the insignificance of the CH_3 group binding to the anion. We also notice that beside the N-H group, the amide bond (CO-N) also plays a role in binding to the anion, as shown in the quantitative analyses in Table S1.

The coupling orientation of KSCN-HCOND₂ dimer

The coupling orientation factor between two modes can be estimated from the DFT calculation results for the dimmers based on Eq. S8. In the orientation factor calculations, the r_{DA} starting point of the CN stretch of SCN⁻ is the center of the CN bond, and that of the ND stretch of HCOND₂ is the position of nitrogen, and that of the OD stretch of D₂O is the position of oxygen. Calculations for isolated molecules and solvated molecules give: $\left(\frac{\kappa_{mean}^{CN/ND}}{\kappa_{mean}^{CN/OD}}\right)_{isolated} = 0.98$, and $\left(\frac{\kappa_{mean}^{CN/ND}}{\kappa_{mean}^{CN/OD}}\right)_{CPCM} = 0.98$. Detailed parameters are provided in table S5. In estimating the energy transfer rate ratio, the refractive indexes of both solutions were taken to be the same.

Table S5. The calculated coupling orientation factors between different modes in four different samples.

sample	mode	method	θ_D (degree)	θ_A (degree)	θ_{DA} (degree)	κ	κ_{mean}
KSCN/ D ₂ O	CN/OD _{stretch}	Isolated	7.50	3.48	11.0	1.99	1.99
		CPCM	2.79	0.633	3.31	2.00	2.00
KSCN/ HCOND ₂	CN/ND _{stretch}	Isolated	4.18	9.15	4.97	1.96	1.96
		CPCM	0.0674	13.3	13.2	1.95	1.95

References

1. Bian, H. T.; Chen, H. L.; Li, J. B.; Wen, X. W.; Zheng, J. R. *J. Phys. Chem. A* **2011**, *115*, 11657-11664.
2. Bian, H. T.; Wen, X. W.; Li, J. B.; Chen, H. L.; Han, S. Z.; Sun, X. Q.; Song, J. A.; Zhuang, W.; Zheng, J. R. *Proc. Natl. Acad. Sci. U. S. A.* **2011**, *108*, 4737-4742.
3. Bostrom, M.; Williams, D. R. M.; Ninham, B. W. *Biophys. J.* **2003**, *85*, 686-694.
4. Orttung, H. W.; Armour, W. R. *J. Phys. Chem.* **1967**, *71*, 2846-2853.
5. Lacourt, A.; Delande, N.; Depaduwa, G. *Anal. Chim. Acta* **1956**, *14*, 100-108.
6. Resa, J. M.; Gonzalez, C.; Landaluce, S. O.; Lanz, J. *J. Chem. Eng. Data* **2000**, *45*, 867-871.
7. Abdel-Azim, Abdel-Azim A.; Munk, P. *J. Phys. Chem.* **1987**, *91*, 3910 - 3914.
8. Checoni, F. R.; Volpe, L. O. P. *J. Solu. Chem.* **2010**, *39*, 259 - 276.
9. Gill, K.B.; Rattan, K.V.; Kapoor, S. *J. Chem. Eng. Data* **2009**, *54*, 1175 - 1178.

10. Popova, S. A.; Orlova, V. T.; Borina, A. F. *Russ. J. Inorg. Chem.* **1993**, *38*, 665-669.